Thermal thickness and evolution of Precambrian lithosphere: A global study

Article *in* Journal of Geophysical Research: Solid Earth · August 2001

DOI: 10.1029/2000JB900439

CITATIONS
682

READS
777

2 authors:

Irina Artemieva
Stanford University
140 PUBLICATIONS **3,780** CITATIONS

SEE PROFILE

Walter D. Mooney
United States Geological Survey Menlo Park California
413 PUBLICATIONS **16,151** CITATIONS

SEE PROFILE

JOURNAL OF GEOPHYSICAL RESEARCH, VOL. 106, NO. B8, PAGES 16,387–16,414, AUGUST 10, 2001

Thermal thickness and evolution of Precambrian lithosphere: A global study

Irina M. Artemieva[1] and Walter D. Mooney
U.S. Geological Survey, Menlo Park, California

Abstract. The thermal thickness of Precambrian lithosphere is modeled and compared with estimates from seismic tomography and xenolith data. We use the steady state thermal conductivity equation with the same geothermal constraints for all of the Precambrian cratons (except Antarctica) to calculate the temperature distribution in the stable continental lithosphere. The modeling is based on the global compilation of heat flow data by *Pollack et al*. [1993] and more recent data. The depth distribution of heat-producing elements is estimated using regional models for ~300 blocks with sizes varying from 1° × 1° to about 5° × 5° in latitude and longitude and is constrained by laboratory, seismic and petrologic data and, where applicable, empirical heat flow/heat production relationships. Maps of the lateral temperature distribution at depths 50, 100, and 150 km are presented for all continents except Antarctica. The thermal thickness of the lithosphere is calculated assuming a conductive layer overlying the mantle with an adiabat of 1300°C. The Archean and early Proterozoic lithosphere is found to have two typical thicknesses, 200–220 km and 300–350 km. In general, thin (~220 km) roots are found for Archean and early Proterozoic cratons in the Southern Hemisphere (South Africa, Western Australia, South America, and India) and thicker (>300 km) roots are found in the Northern Hemisphere (Baltic Shield, Siberian Platform, West Africa, and possibly the Canadian Shield). We find that the thickness of continental lithosphere generally decreases with age from >200 km beneath Archean cratons to intermediate values of 200 ± 50 km in early Proterozoic lithosphere, to about 140 ± 50 km in middle and late Proterozoic cratons. Using known crustal thickness, our calculated geotherms, and assuming that isostatic balance is achieved at the base of the lithosphere, we find that Archean and early Proterozoic mantle lithosphere is 1.5% less dense (chemically depleted) than the underlying asthenosphere, while middle and late Proterozoic subcrustal lithosphere should be depleted by ~0.6–0.7%. Our results suggest three contrasting stages of lithosphere formation at the following ages: >2.5 Ga, 2.5–1.8 Ga, and <1.8 Ga. Ages of komatiites, greenstone belts, and giant dike swarms broadly define similar stages and apparently reflect secular changes in mantle temperature and, possibly, convection patterns.

1. Introduction

Seismic tomography shows that the continental lithosphere of many Archean (>2.5 Ga) shields commonly exceeds 200–300 km, whereas the lithosphere of post-Archean (<2.5 Ga) crust is only 100–200 km thick [e.g., *Ritsema and van Heijst*, 2000; *van der Lee and Nolet*, 1997; *Ekström et al*., 1997; *Polet and Anderson*, 1995; *Grand*, 1994; *Zhang and Tanimoto*, 1993]. For example, the correlation between the age of a craton and *S* wave velocities in the mantle lithosphere [*Polet and Anderson*, 1995] suggests that Archean and early Proterozoic cratons typically have lithospheric roots that are 240–280 km thick, whereas the lithosphere beneath middle and late Proterozoic terraines is only ~150 km thick (for 1% V_s anomaly; for 0.5% V_s anomaly the lithosphere is ~60 km thicker). *Jordan* [1975, 1979, 1988] proposed the existence of a naturally buoyant tectosphere that may be 400 km thick beneath old cratons. In contrast, studies of pressure-temperature (P-T) relations for mantle xenoliths suggest only ~200–220 km thickness for the Archean lithosphere in South Africa, eastern Siberia, the Baltic Shield, and North America [e.g., *Boyd*, 1984; *Boyd et al*., 1985; *Mackenzie and Canil*, 1997; *Rudnick et al*., 1998; *Rudnick and Nyblade*, 1999; *Kopylova et al*., 1999; *Kukkonen and Peltonen*, 1999]. In these studies it is assumed that the xenolith P-T data reflect equilibrium to a conductive geotherm, rather than having geotherms perturbed by kimberlite magmatism. Thus these studies provide a minimum estimate of lithospheric thickness in Archean shields.

In this study we estimate the thermal thickness of the Precambrian lithosphere and compare it to the lithospheric thickness as estimated from global and regional seismic tomography and from P-T data derived from lithospheric xenoliths. In accord with *McNutt* [1990] and *Jaupart and Mareschal* [1999] we assume that the thickness of the mechanical lithosphere is proportional to the thickness of the conductive thermal boundary layer z_1 (Figure 1) and define the base of the thermal lithosphere z_2 as the intersection of a geotherm with a mantle abiabat T_m = 1300°C. High-temperature dislocation relax-

[1]Now at Department of Earth Sciences, Uppsala University, Uppsala, Sweden.

Paper number 2000JB900439.

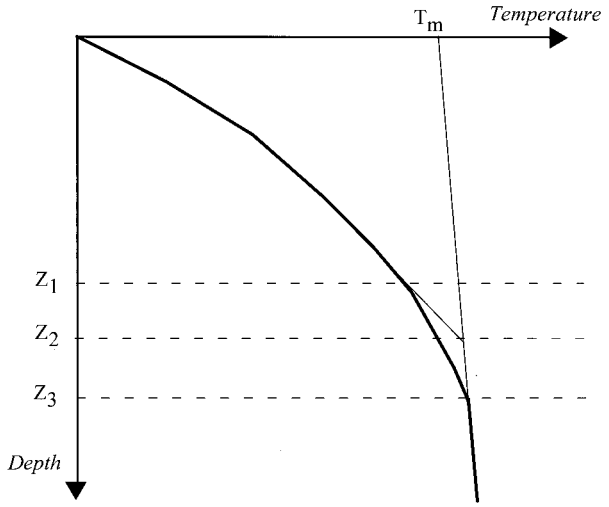

Figure 1. Relationship between the thermal and seismic lithospheric thicknesses [after *Jaupart and Mareschal*, 1999] (with permission from Elsevier Science), where z_1 is thickness of the conductive thermal boundary layer where heat transport is achieved by conduction, z_2 is the base of the thermal lithosphere at the intersection of the conductive geotherm with the mantle abiabat T_m, and z_3 is the total thickness over which temperature contrasts persist with the surrounding mantle, the base of the seismic lithosphere, and the top of the convecting mantle.

ation and partial melting decrease seismic velocities [*Anderson and Sammis*, 1970; *Sato et al*., 1989]. However, because lithospheric temperature changes gradually with depth, the base of the seismic lithosphere is diffuse, and global seismic tomography based on surface waves will generally show velocity anomalies to greater depth, down to the top of the convective mantle, z_3, deeper than z_2. *Jaupart et al*. [1998] discuss thermal conditions at the base of the continental lithosphere and calculate the depth difference between the conductive thermal boundary layer and the top of the convective mantle to be ~40 km.

We calculate the thermal thickness of the Precambrian continental lithosphere, considering it as a conductive layer overlying the convective adiabatic mantle. This study is facilitated by global databases for heat flow [*Pollack et al*., 1993] and crustal structure [*Mooney et al*., 1998]. The thermal state of the continental lithosphere has been addressed in numerous publications (Table 1). Most of these were individual studies of South Africa, the Baltic Shield, the Indian Shield, Australia, and North America. There are relatively few publications on the thermal state of the lithosphere in China, South America, and Siberia. One important motivation for our study is the fact that problems arise in comparing the estimates of lithospheric thermal thickness published for different Precambrian regions since different values of heat production and thermal conductivity were assumed in these model calculations.

In this study we calculate the thermal state of the lithosphere for all Precambrian cratons (except Antarctica) using consistent assumptions for depth distributions of thermal parameters. This approach permits quantitative comparison of models of lithospheric geotherms and lithospheric thermal thickness, even if the calculated values contain systematic biases. Such a bias could arise, for example, if the true values of heat production or thermal conductivity in the lower crust or lithospheric mantle are different from those assumed here. The only previous global study of the thermal state of the continental lithosphere [*Pollack and Chapman*, 1977] is more than 20 years old. It was based on a degree-12, spherical harmonic representation of global surface heat flow that provided a smoothed and generalized estimate of lithospheric thickness. The large number of new heat flow measurements now available make possible the approach taken in this paper.

We consider eight of the nine Precambrian cratons (Figure 2): the East European (including Baltic and Ukranian Shields), Siberian, Indian, Australian, African, South American, North American, and Cathaysian (Asiatic) Cratons. No geothermal data are available for the Antarctic Craton. In some cases, the thermal regime of Phanerozoic regions adjacent to Precambrian cratons is shown on our maps as in East Africa. No geothermal modeling was carried out for these regions, and instead we used published geotherms based on petrologic estimates and nonsteady state geothermal calculations [e.g., *Decker*, 1995; *Lachenbruch and Sass*, 1977; *Le Pichon et al*., 1997; *Mechie et al*., 1994; *Polyakov et al*., 1988].

2. Methodology and Estimation of Thermal Properties of Precambrian Crust and Lithosphere

2.1. Method

Most heat flow measurements in Archean and Proterozoic regions are located in areas that have not experienced a major tectonic event since the end of the Precambrian [*Nyblade and Pollack*, 1993]. Therefore, in these regions the thermal struc-

Table 1. Previous Studies of the Thermal State of Precambrian Lithosphere[a]

Craton	Precambrian Geotherms Studies	Lithosphere Thermal Thickness Studies[b]
Global	11, 16, 45	45
Africa	1, 12, 31	1, 12, 13, 32, 40
Australia	14, 21, 47, 48	15, 21, 22, 41
China	50	50
India	23–25, 38, 39, 49	25, 38, 39
Europe	2, 3, 5, 7, 8, 10, 34, 35, 42	2, 5, 6, 8, 34, 35, 42, 43
Siberia	19, 20	6, 20
North America	4, 9, 17, 18, 29, 30, 33, 36, 37, 44, 46	28, 29, 37
South America	26, 27	

[a]Studies: 1, *Ballard and Pollack* [1987]; 2, *Balling* [1995]; 3, *Baumann and Rybach* [1991]; 4, *Bodri and Jessop* [1989]; 5, *Burianov et al*. [1985]; 6, *Cermak* [1982]; 7, *Cermak and Bodri* [1986]; 8, *Cermak and Bodri* [1995]; 9, *Cermak and Jessop* [1971]; 10, *Cermak et al*. [1989]; 11, *Chapman* [1986]; 12, *Chapman and Pollack* [1974]; 13, *Chapman and Pollack* [1977]; 14, *Cull and Conley* [1983]; 15, *Cull et al*. [1991]; 16, *Davies and Strebeck* [1982]; 17, *Drury* [1985]; 18, *Drury et al*. [1987]; 19, *Duchkov and Sokolova* [1995]; 20, *Duchkov et al*. [1987]; 21, *Ferguson et al*. [1979]; 22, *Griffin et al*. [1987]; 23, *Gupta* [1993]; 24, *Gupta et al*. [1987]; 25, *Gupta et al*. [1991]; 26, *Hamza* [1982a, 1982b]; 27, *Hurter and Pollack* [1996]; 28, *Jaupart et al*. [1998]; 29, *Jaupart and Mareschal* [1999]; 30, *Jessop and Lewis* [1978]; 31, *Jones* [1992]; 32, *Jones* [1988]; 33, *Judge* [1978]; 34, *Kukkonen and Peltonen* [1999]; 35, *Kutas et al*. [1989]; 36, *Mareschal* [1991]; 37, *Mareschal et al*. [2000a]; 38, *Negi et al*. [1986]; 39, *Negi et al*. [1987]; 40, *Nicolaysen et al*. [1981]; 41, *O'Reilly and Griffin* [1985]; 42, *Pasquale et al*. [1990]; 43, *Pasquale et al*. [1991]; 44, *Pinet et al*. [1991]; 45, *Pollack and Chapman* [1977]; 46, *Russell and Kopylova* [1999]; 47, *Sass and Lachenbruch* [1979]; 48, *Sass et al*. [1976]; 49, *Singh and Negi* [1982]; 50, *Wang* [1996].

[b]Values given in Table 6.

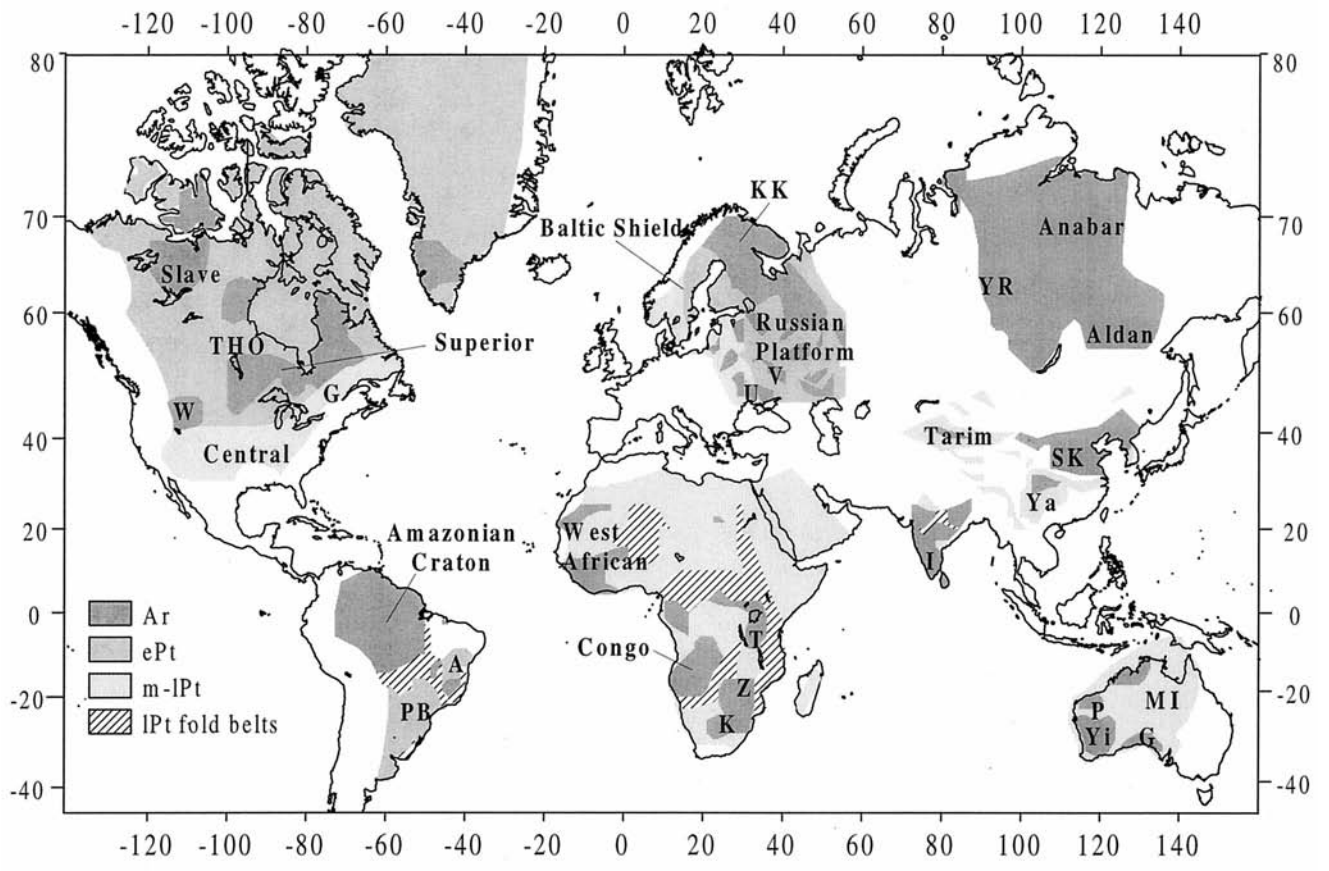

Figure 2. Archean (Ar) and Proterozoic (ePt, early Proterozoic; m-lPt, middle to late Proterozoic) regions of the world (based on data compiled from *Goodwin* [1996]) and adjacent tectonic structures of different ages considered in the present study. A, Atlantic Shield; G, Gawler Craton; Gr, Grenville Province; I, Indian Shield; KK, Kola-Karelian province; K, Kaapvaal Craton; MI, Mount Isa Orogen; P, Pilbara Block; PB, Parana Basin; SK, Sino-Korean Craton; T, Tanzanian Craton; THO, Trans-Hudson Orogen; U, Ukrainian Shield; V, Voronezh Massif; W, Wyoming Province; Ya, Yangtze Craton; Yi, Yilgarn; YR, Yenisey Ridge; Z, Zimbabwe Craton.

ture of the lithosphere can be approximated by the steady state solution of the thermal conductivity equation:

$$\nabla^2 T = -A/k \tag{1}$$

with boundary conditions at the surface given by

$$T|_{z=0} = 0$$

$$Q_0 = -k \frac{\partial T}{\partial z},$$

where Q_0 is the near-surface heat flow, T is temperature, $k = k(z)$ is thermal conductivity as a function of depth (z), and $A = A(z)$ is the heat production as a function of depth. The solution of this boundary value problem permits the calculation of temperatures within the crust and lithospheric mantle. Such calculations are constrained primarily by surface heat flow measurements and the associated distribution of thermal parameters (thermal conductivity and heat production) within the crust and the lithospheric mantle. Data on near-surface heat flow are based on measurements of thermal gradient and conductivity in boreholes chosen in this study to avoid water circulation in permeable rocks higher in the crust. Data on crustal structure and composition are used to constrain the distribution of thermal parameters with depth, which is discussed in sections 2.3 and 2.4.

For most of the Precambrian cratons the distribution of heat flow and crustal structure data are insufficient for two-dimensional (2-D) modeling, and so 1-D estimates of the lithospheric thermal structure were made. This is a reasonable approximation, as differences between the results of 1-D and 2-D modeling mostly occur in the areas with strong contrasts in crustal thermal parameters over a short distance [*Jaupart*, 1983]. Temperature differences due to such contrasts usually do not exceed 50–100°C at Moho depth, which is about the accuracy of the geothermal modeling.

2.2. Heat Flow Data

The heat flow data that are considered most reliable (as discussed below) were compiled and analyzed for the Precambrian cratons. Most of the geothermal data used in this study were derived from the global heat flow compilation of *Pollack et al.* [1990, 1993]. The total number of worldwide heat flow measurements in this database is close to 300 for Archean and ~1000 for Proterozoic crust [*Nyblade and Pollack*, 1993]. These data were supplemented by other heat flow data for the Siberian Platform (10 measurements from the Tunguska de-

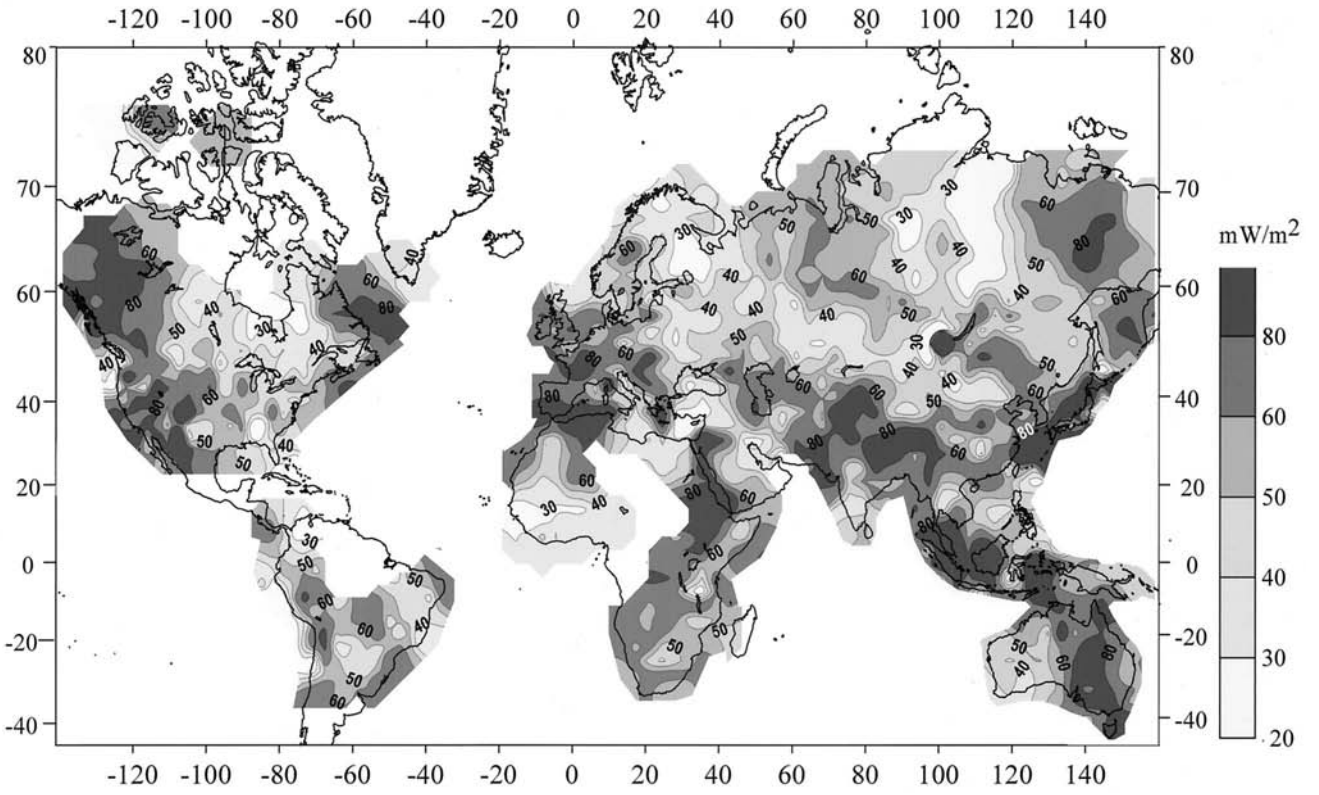

Figure 3. Surface heat flow updated from the *Pollack et al*. [1990, 1993] database presented with a 10° × 10° interpolation. We modeled only data from Precambrian regions assuming steady state thermal conditions.

pression [*Duchkov et al*., 1987]), Baltic Shield (54 new measurements in Sweden (Swedish Geothermal Resources Borehole Data Summary, unpublished, 1994)), Canadian Shield (new heat flow data for the Abitibi belt, the Grenville Province, and the Trans-Hudson Orogen [*Drury and Taylor*, 1987; *Guillou et al*., 1994; *Guillou-Frottier et al*., 1995, 1996; *Mareschal et al*., 1999, 2000a; *Jaupart and Mareschal*, 1999; J.-C. Mareschal, personal communication, 1998]), Brazil (about 50 new measurements in the Parana Basin [*Hurter and Pollack*, 1996]), and Africa (12 heat flow measurements in Lesotho and four in the Tanzanian Craton [*Jones*, 1992; *Nyblade*, 1997]). Heat flow data for India were updated with recent high-quality studies in the Indian Shield and especially in the Deccan Province [*Gupta et al*., 1993; S. Rao, personal communication, 1998]). Figure 3 shows a 10° × 10° interpolation of the surface heat flow for the Precambrian; the sites of heat flow measurements are shown in Figure 4.

Here we used only the most reliable heat flow values, applying criteria discussed by *Pollack et al*. [1993] and *Cull* [1982]. For example, heat flow data from shallow boreholes potentially affected by a groundwater circulation and data obtained by nonconventional methods (mostly from Brazil) were excluded from this study. Heat flow data for West Africa are sparse, but a recent reassessment of these data indicates that the measured values are reliable (J. Behrendt, personal communication, 2000). All original heat flow data were analyzed, as far as possible, for potential regional perturbations (e.g., long-term temperature variations due to climatic changes, such as Pleistocene glaciations). Paleoclimatic corrections to surface heat flow data were made using standard procedures [*Beck*, 1977; *Powell et al*., 1988], and in the northernmost areas these can be as large as 15–20 mW m^{-2} [e.g., *Balling*, 1995].

For each of the Precambrian cratons, surface heat flow data were analyzed separately for geologic provinces of different ages (Figure 5). Crustal age was estimated from the summary of *Goodwin* [1996]. We assume that these ages of the crust give the minimum age of the subcrustal lithosphere. This assumption is supported by recent geochemical studies that suggest that the crust and mantle lithosphere are of about the same geologic age [*Richardson et al*., 1993; *Pearson*, 1999].

Each geologic province was subdivided into smaller blocks with similar heat flow values and crustal structure, yielding ~300 blocks, with sizes varying from 1° × 1° to about 5° × 5°. The average surface heat flow was calculated for each block; in some cases a few extreme heat flow values were excluded as these presumably were affected by nonconductive heat transfer such as groundwater circulation.

2.3. Thermal Conductivity

Seismic data from the global crustal database of the U.S. Geological Survey were used to define an upper, middle, and lower crust in order to constrain typical models of the depth distribution of thermal parameters for the heat flow provinces. In regions where the number of seismic profiles is insufficient, averaged seismic models of crustal structure based on the statistical analysis of crustal structure of regions with a similar tectonic setting and crustal age were used. *Mooney et al*. [1998] present a location map of the seismic profiles used.

Laboratory measurements of thermal conductivity on rock samples from upper crustal sedimentary and crystalline rocks

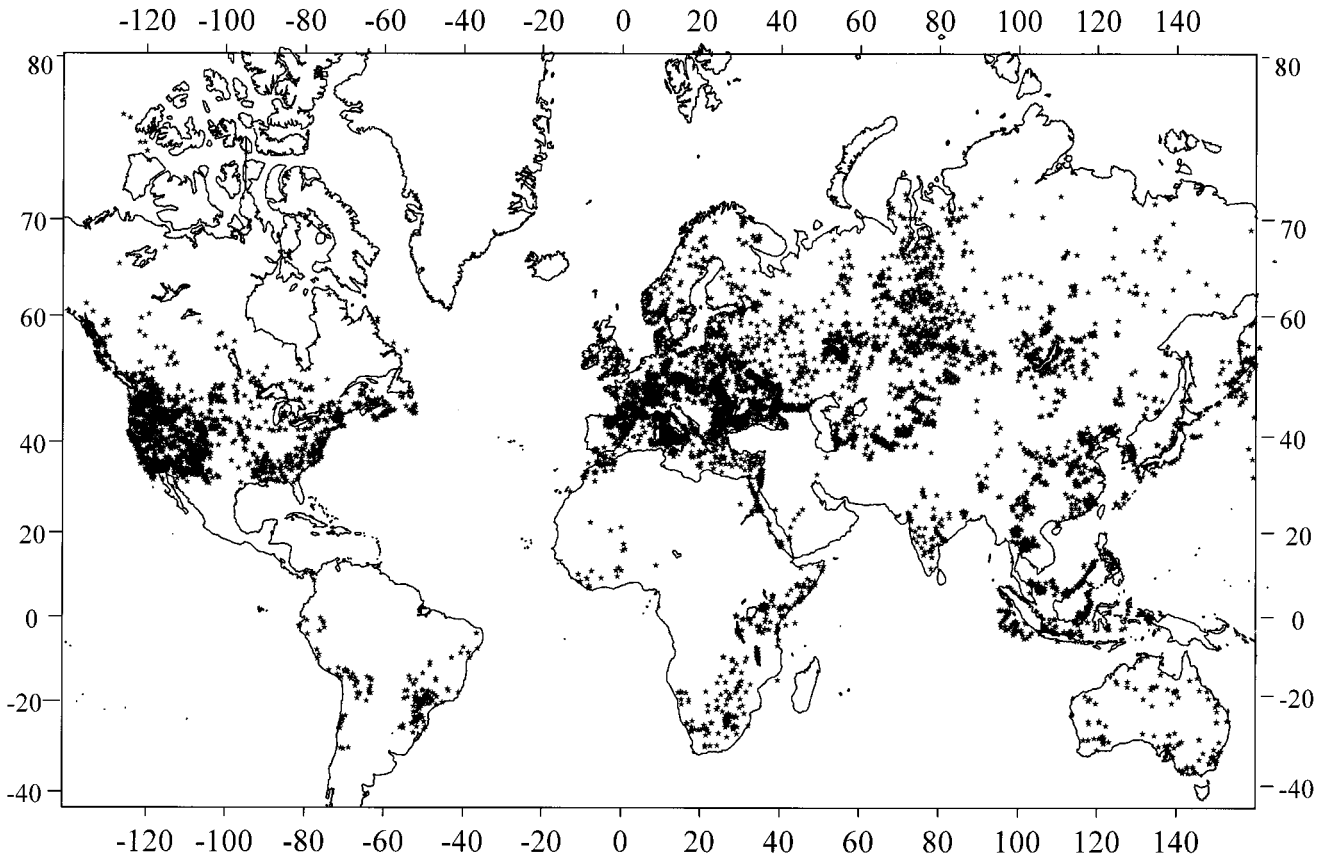

Figure 4. Locations of continental heat flow measurements used in this study. The database of *Pollack et al.* [1993] has been supplemented by recently determined values from Russia, Canada, Sweden, Africa, Brazil, and India (see text).

from the study regions were used to constrain the depth distributions of thermal conductivity. The temperature and pressure dependence of thermal conductivity was accounted for in the modeling. At crustal temperatures the conductivity of most rocks decreases with increasing temperature. For the upper crust the following relation [e.g., *Cermak and Rybach*, 1982] was used:

$$k = k_0/(1 + cT), \tag{2}$$

where k_0 is the thermal conductivity at 0°C and near-surface pressure conditions and c is a material constant (in the range 0 to 0.003°C^{-1}), determined by experimental studies on rock samples. In the present study, c was assumed to be 0.001°C^{-1} for the upper crust. The pressure effect, which is relatively small [*Seipold*, 1992], was not accounted for separately, but following *Balling* [1995], it was included in depth variations of conductivity due to composition and temperature. Variations of thermal conductivity with depth in the crust are much less significant than variations in heat production (Table 2).

We assumed that the thermal conductivity of the lower crust is constant (Table 2). Laboratory measurements confirm that at temperatures of 200–600°C, which are typical for Precambrian lower crust, the thermal conductivity of rocks is almost constant and equal to 2.0 W m^{-1} K^{-1} [*Seipold*, 1992]. For lithospheric mantle we assume peridotitic composition and a constant conductivity of 4.0 W m^{-1} K^{-1} [*Schatz and Simmons*, 1972; *Scharmeli*, 1979]. We present a sensitivity analysis of our model assumptions in section 2.5.

2.4. Heat Production in the Crust

The depth distribution of radioactive heat production in the crust is critical for thermal modeling. No single technique for estimating the crustal depth distribution of radiogenic heat production $A(z)$ has proven to be consistently accurate, so we use a combination of approaches (discussed below) that accords with present ideas on crustal radioactivity. The number of models for the depth distribution of radiogenic heat production used here is too numerous (more than 500) to describe each model in detail. We limit ourselves to a description of the general ideas that were used to constrain these models. A summary of the numerical values of the thermal properties of the crust and the upper mantle used is presented in Table 2. An additional constraint is that the estimated mantle heat flow should not exceed the lowest measured surface heat flow in a region.

2.4.1. Experimental data. Laboratory measurements of heat production in sedimentary rocks and Precambrian basement rocks form the basis for models of heat production in the upper crust. The values of heat production assumed for the sedimentary cover are based on published measurements for the regions of interest. Values of A_0 (heat production for near-surface basement rocks) for each of ~300 crustal blocks considered here were based on average and, where possible, area-weighted values reported for the regions of study [e.g., *Ashwal et al.*, 1987; *Ballard et al.*, 1987; *Guillou-Frottier et al.*, 1995; *Hamza*, 1982b; *Jones*, 1987; *Kremenetsky et al.*, 1989;

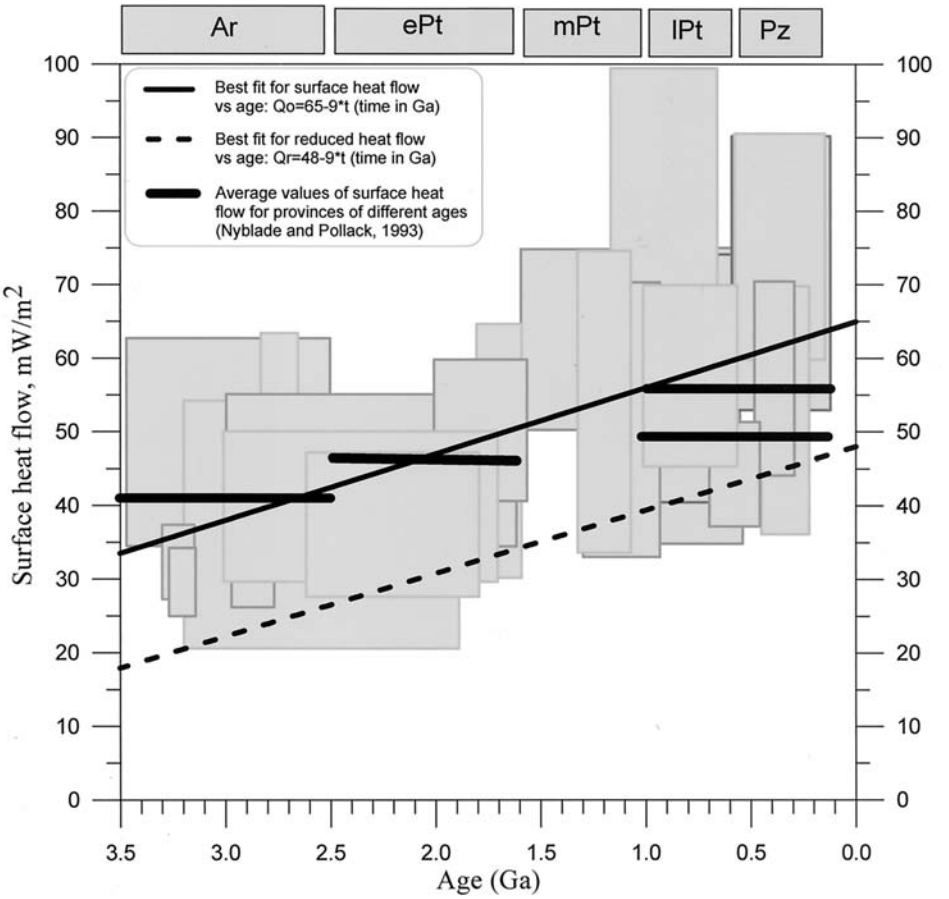

Figure 5. Surface heat flow versus crustal age. Shaded rectangles refer to different heat flow provinces, the horizontal size gives the range in age [*Goodwin*, 1996], and the vertical size shows surface heat flow variations. Mean heat flow estimates from *Nyblade and Pollack* [1993] are shown, as are the best fitting curves for both surface and reduced heat flow. Pz, Paleozoic.

Kukkonen, 1989; *Kutas et al*., 1989; *Rao et al*., 1976; *Rozen*, 1992; *Vernik et al*., 1985].

2.4.2. Heat flow/heat production for Precambrian cratons. Where heat flow/heat production data show a clear linear trend, we used the concept of "heat flow provinces" [*Roy et al*., 1968] and the linear relationship within a heat flow province between mean surface heat flow Q_0 and heat production [e.g., *Birch et al*., 1968; *Lachenbruch*, 1970]:

$$Q_0 = Q_r + DA_0, \quad (3)$$

where Q_r is the "reduced" heat flow, A_0 is the heat production measured in near-surface rocks, and D is the characteristic depth over which most of the heat-producing elements (HPEs) are distributed. In some regions, where conductivity and crustal heat production are heterogeneous on a small scale, heat flow correlates poorly with heat production and the linear heat flow/heat production relationship is invalid [e.g., *England et al*., 1980; *Jaupart*, 1983; *Jaupart and Mareschal*, 1999; *Mareschal et al*., 2000a, 2000b]. Nonetheless, reduced heat flow is

Table 2. Thermal Properties of the Precambrian Crust and Lithosphere as Assumed in This Study

Layer	Depth Range, km	V_p, km s^{-1}	Thermal Conductivity k, W m^{-1} K^{-1}	c (Temperature Correction to k) $k = k_0/(1 + cT)$	Heat Production A, μW m^{-3}	Basis for Assumed Heat Production Values
Sedimentary cover	0–10	3.0–5.6	0.5–4.0	···	0.7–1.3	laboratory data for rocks samples
Upper crust	0–25	5.6–6.0	2.5–3.0	0.001	0.4–6.7	laboratory data, "heat flow provinces," exponential decrease with depth, exposed crust
		6.0–6.5	2.6–2.8	0.001	0.4–0.5	assumed globally
Middle crust	20–40	6.5–7.0	2.0–2.5	···	0.2–0.4	assumed globally
Lower crust	30–50	7.0–7.5	2.0	···	0.1	assumed globally
Lithospheric mantle	>35–50	>7.9	4.0	···	0.01	assumed globally
		>8.3	4.0	···	0.004	assumed globally

Table 3. Heat Flow/Heat Production Relationships for the Precambrian Cratons[a]

Craton	Ar-ePt		mPt-lPt		References[b]
	Q_r, mW m^{-2}	D, km	Q_r, mW m^{-2}	D, km	
East European	22–32.8	4.7–13.0	19.8–35.0	6.6–15.6	1, 2, 4, 5, 24–26, 29, 31, 36
Siberian	13.1–18.5	9.7–13.5	...	...	1, 10
North American	26.5–42.1	4.6–13.6	30.5–33.9	6.1–8.8	1, 6, 9, 11, 12, 20, 23, 27, 30
South American	28–37	4.5–13.1	37.5–53.2	4.7–11	1, 16, 17, 37
Australian	26.5–32.3	3.3–4.5	27–55	5.5–11.1	1, 19, 35
African	11–31.1	1.9–8.0	34–50	5.5–11.0	1, 3, 7, 8, 18, 21, 22, 28, 34
Indian	20–33	7.5–11.5	33–38	15	1, 13–15, 32, 33

[a]Ar, Archean; ePt, early Proterozoic; mPt, middle Proterozoic; lPt, late Proterozoic.
[b]References: 1, this study; 2, *Arshavskaya* [1979]; 3, *Ballard et al*. [1987]; 4, *Balling* [1990]; 5, *Balling* [1995]; 6, *Cermak and Jessop* [1971]; 7, *Chapman and Pollack* [1974]; 8, *Chapman and Pollack* [1977]; 9, *Drury* [1985]; 10, *Duchkov et al*. [1994]; 11, *Fountain et al*. [1987]; 12, *Guillou-Frottier et al*. [1996]; 13, *Gupta and Sharma* [1979]; 14, *Gupta et al*. [1991]; 15, *Gupta et al*. [1993]; 16, *Hamza* [1982a]; 17, *Hamza* [1982b]; 18, *Hart et al*. [1981]; 19, *Jaeger* [1970]; 20, *Jessop and Lewis* [1978]; 21, *Jones* [1987]; 22, *Jones* [1988]; 23, *Judge* [1978]; 24, *Kukkonen* [1989]; 25, *Kutas et al*. [1989]; 26, *Malmquist et al*. [1983]; 27, *Mareschal et al*. [1989]; 28, *Nyblade et al*. [1990]; 29, *Pinet and Jaupart* [1987]; 30, *Pinet et al*. [1991]; 31, *Rao and Jessop* [1975]; 32, *Rao et al*. [1976]; 33, *Rogers and Callahan* [1987]; 34, *Sass and Behrendt* [1980]; 35, *Sass and Lachenbruch* [1979]; 36, *Swanberg et al*. [1974]; 37, *Vitorello et al*. [1980].

roughly uniform in heat flow provinces of the same age [*Jaupart*, 1983]. As it is unlikely that reduced heat flow is affected by nonvertical heat conduction in all provinces, equation (3) will still yield reasonable estimates for average heat flow at midcrustal levels.

Recent seismological studies [*Durrheim and Mooney*, 1994] suggest that the structure and composition of Archean crust may differ from that of middle and late Proterozoic crust. For this reason, heat flow/heat production data for Archean and early Proterozoic (1.7–3.5 Ga) and mid-late Proterozoic (0.6–1.7 Ga) regions were considered separately.

Table 3 and Figure 6 summarize the range of Q_r and D for different Precambrian regions as estimated in this study and compiled from the literature. For the North American craton we use only estimates based on heat flow data corrected for paleoclimatic variations. These corrections range from 2 to 12 mW m^{-2} [*Pinet et al*., 1991; *Guillou-Frottier et al*., 1995]. Too few geothermal data are available for the Cathaysian Craton to permit an independent interpretation of heat flow/heat production relationships. For this craton we used the values of A_0 and D reported by *Wang* [1996] for five tectonic provinces in China.

An analysis of heat flow/heat production relationships for seven of the nine main Precambrian cratons (except the Cathaysian and Antarctica) suggests colder mantle beneath the Archean and early Proterozoic regions and a more shallow enrichment of HPEs in the crust. Variations of reduced heat flow with geologic age are shown in Figure 7 for each Precambrian craton. There is a well-pronounced trend indicating an increase of reduced heat flow (i.e., mainly mantle heat flow) with decreasing age, from 10–30 mW m^{-2} in the Archean crust to 30–45 mW m^{-2} in late Proterozoic crust. The only region that deviates from the general trend is southern Africa, which is topographically higher than other Precambrian terrains. Higher values of reduced heat flow in this region are likely to reflect higher values of mantle heat flow (possibly plume-related [e.g., *Lithgow-Bertelloni and Silver*, 1998]), which can also produce the observed topography.

We found no systematic global variation of D values with age. However, within each craton the value of D usually in-

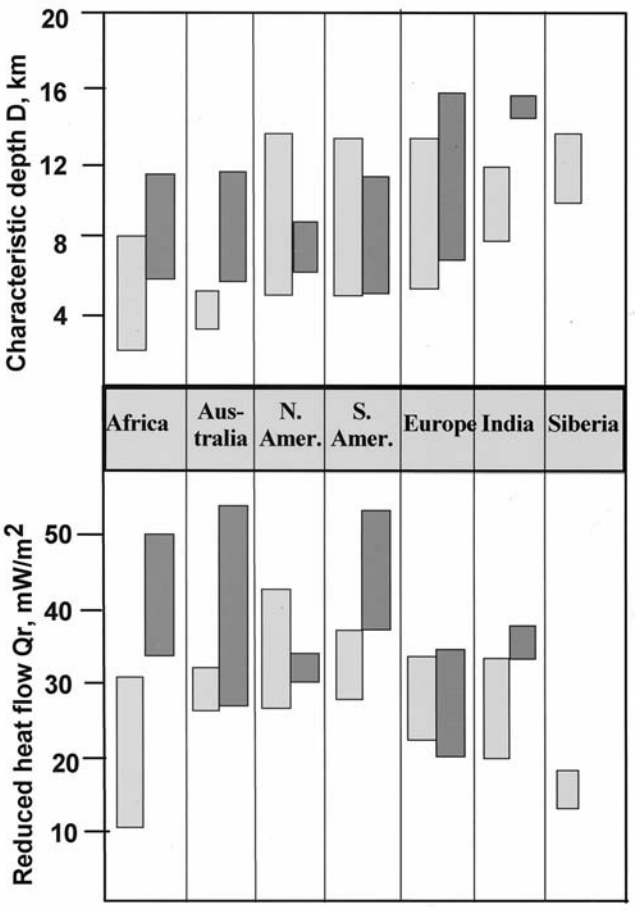

Figure 6. Characteristic depth D and reduced heat flow Q_r of the heat flow/heat production relationship (equation (3)). Light shading corresponds to Archean and early Proterozoic cratons, and dark shading corresponds to middle and late Proterozoic cratons. We find that Archean and early Proterozoic cratons and the middle and late Proterozoic cratons have many characteristics in common, and thus we have grouped these cratons together, rather than dividing cratons at the Archean-Proterozoic boundary.

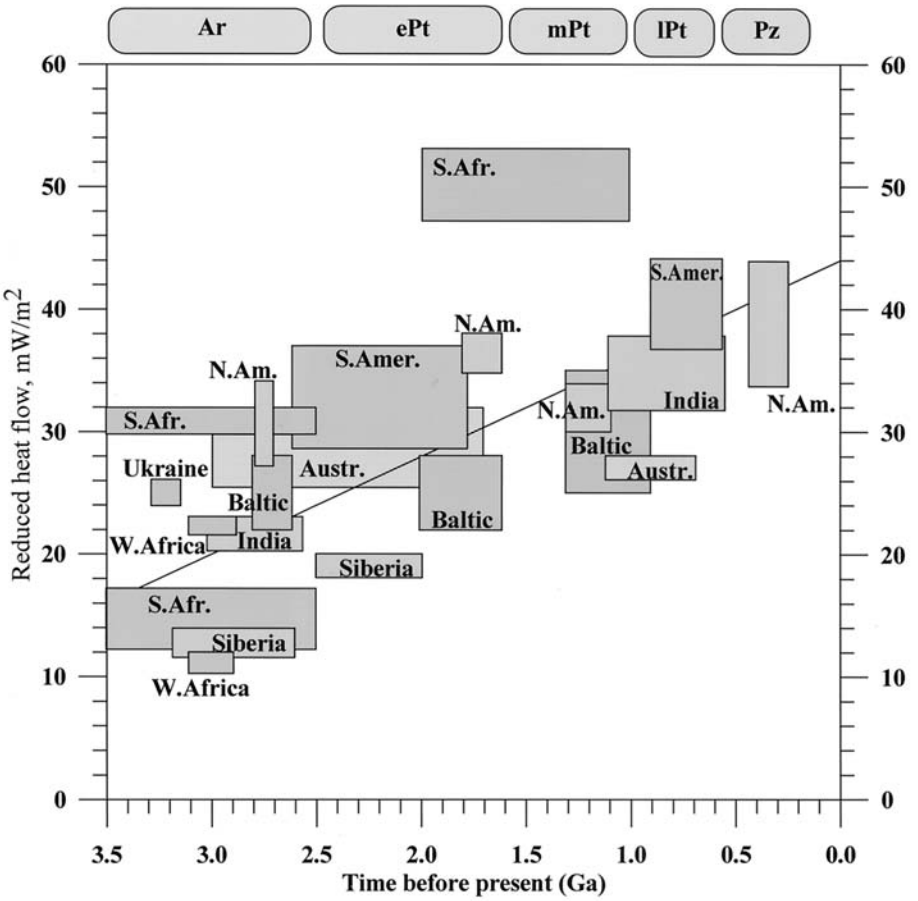

Figure 7. Reduced heat flow versus age. Boxes correspond to individual cratons. The age ranges are based on the data of *Goodwin* [1996], whereas the span along the vertical axis reflects variations in estimated values of the reduced heat flow obtained by different authors. Best fit line for variations of reduced heat flow with age for all continents is the line $Q_r = 44–8*t$ (time in Ga). Austr., Australia; Baltic, Baltic Shield; India, Indian Shield; N. Am., North America; S. Afr., South Africa; S. Amer., South America; Siberia, Siberian Craton; Ukraine, Ukrainian Shield; W. Africa, West African Craton.

creases with the age of individual terrains and can vary from 2–5 km in Archean cratons (Kaapvaal Craton, Western Australia, Superior Province) to ~15 km in some Proterozoic crust of Eurasia and North America. Thus the commonly cited value of $D = 10$ km seems to be an underestimate for parts of the Precambrian of Europe, Siberia, and India, whereas it is often an overestimate for the Precambrian crust of South America, South Africa, and Australia.

2.4.3. Exponential decrease of heat production with depth. In a global study such as this, simple and often-used modeling assumptions are needed even if some studies indicate that the real Earth is locally more complex [cf. *Ketcham*, 1996]. For this reason, we use the well-known assumption of an exponential decrease in heat production with depth [*Lachenbruch*, 1970], $A(z) = A_0 \exp(-z/D)$ for the crystalline upper crust, with a variable thickness D as described in section 2.4.2 (Table 3). A detailed discussion of the distribution of HPE within the crust of the Arizona Basin and Range Province based on measured values of heat production from exposures of the upper and middle crust is presented by *Ketcham* [1996]. He concludes that a model with an exponential $A(z)$ decrease will underestimate heat production in the middle and lower crust in his study area. In recognition of this, we use an exponential decrease in heat production with depth only for the upper crust (see Table 2). This assumption, combined with average seismic models of crustal structure for each of about 300 blocks modeled, was used to constrain the vertical distribution of heat production for each of the blocks. Some exceptions were made from the exponential distribution of $A(z)$ in the case of low-velocity zones in the crust that indicate a greater thickness of felsic, radiogenic-enriched rocks, but this did not significantly change the general pattern of decreasing radiogenic heat production with depth.

2.4.4. Correlation between seismic velocity and heat production. The selection of possible crustal rock types and their heat production values was based on crustal seismic information [*Christensen and Mooney*, 1995; *Rudnick and Fountain*, 1995]. We assumed that, in general, crustal layers with higher velocities have lower heat production (see Table 2) but did not use an empirical linear relationship between experimentally measured heat production and compressional velocity, as suggested by *Rybach and Buntebarth* [1984]. Some experimental results [e.g., *Fountain*, 1986; *Kern and Siegesmund*, 1989] imply that heat production may not be reliably predicted from seismic velocity.

2.4.5. Relation between surface and reduced heat flow. We evaluated the correlation between surface and reduced heat flow for regions of different geologic ages (Figure 8). For

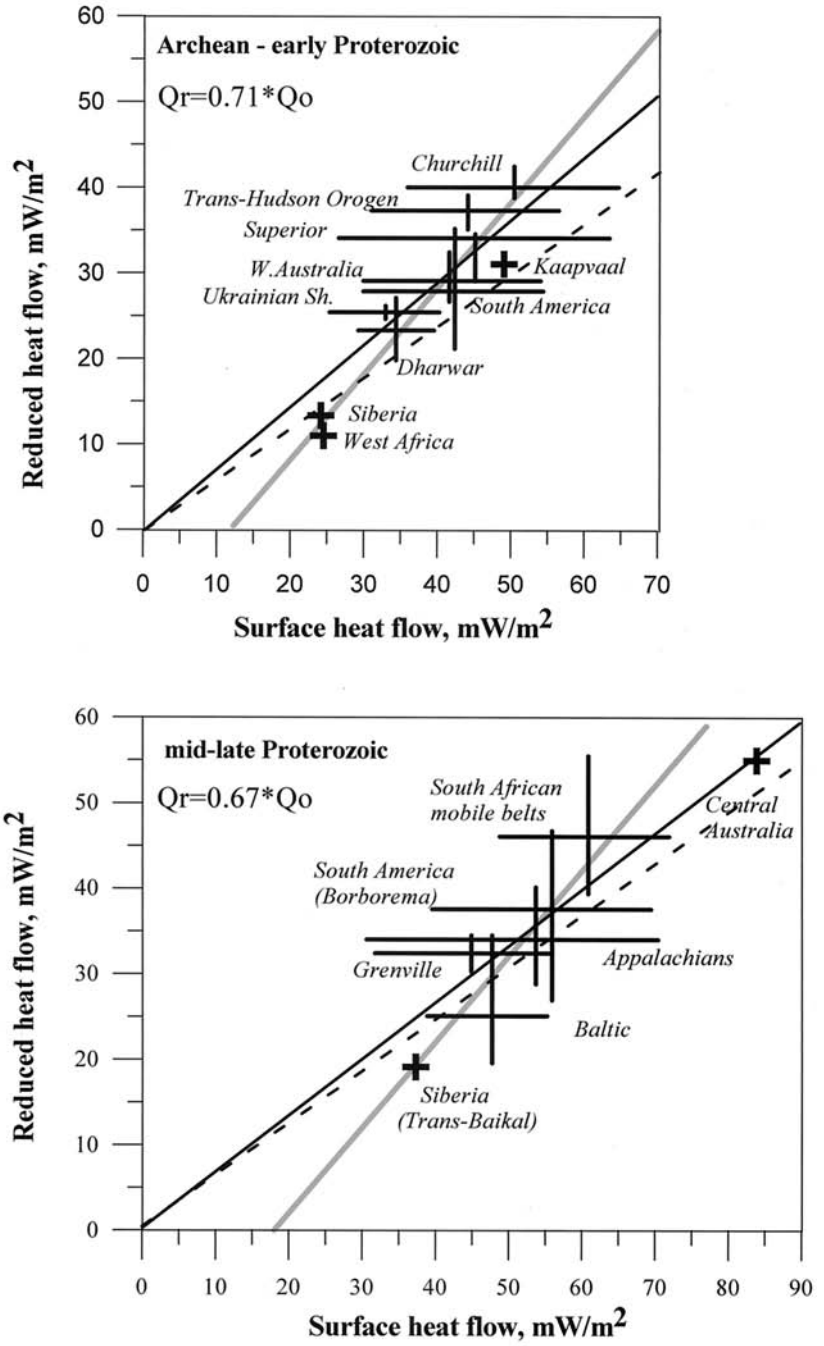

Figure 8. Reduced heat flow versus surface heat flow for different Archean–early Proterozoic and mid-late Proterozoic regions. The horizontal bars show variations of surface heat flow within each of the regions, and the vertical bars give the span in the estimates of the reduced heat flow reported for them by different authors (for references, see Table 3). Solid lines, best linear fit to the data; dashed lines, $Q_0 = 0.60*Q$ [*Pollack and Chapman*, 1977]. Shaded lines imply that the contribution of the upper crustal (D) layer to the surface heat flow is ~12 mW m^{-2} in Archean–early Proterozoic regions and 18 mW m^{-2} in mid-late Proterozoic regions.

those regions where the linear heat flow/heat production relationship is valid (Table 3), ~30% of the mean surface heat flow arises from near-surface radiogenic sources for the Precambrian crust. This is equivalent to saying that the reduced heat flow (Q_r) is ~70% of the total measured heat flow (Figure 8). This value was used to control our models of the total crustal radioactivity and thus the crustal contribution to the observed heat flow. However, in the individual crustal blocks the contribution of the crust to the surface heat flow values can have a wider variation from ~25% to 75%, as suggested by *Morgan* [1985] and this study. Our result for Precambrian crust differs from the suggestion of *Pollack and Chapman* [1977] that on average, 40% of surface heat flow arises from near-surface radiogenic sources. The results (Figure 8) also imply that on average, the contribution of the upper crustal layer to the surface heat flow is about 12 mW m^{-2} in Archean–early Proterozoic regions and 18 mW m^{-2} in mid-late Proterozoic terrains.

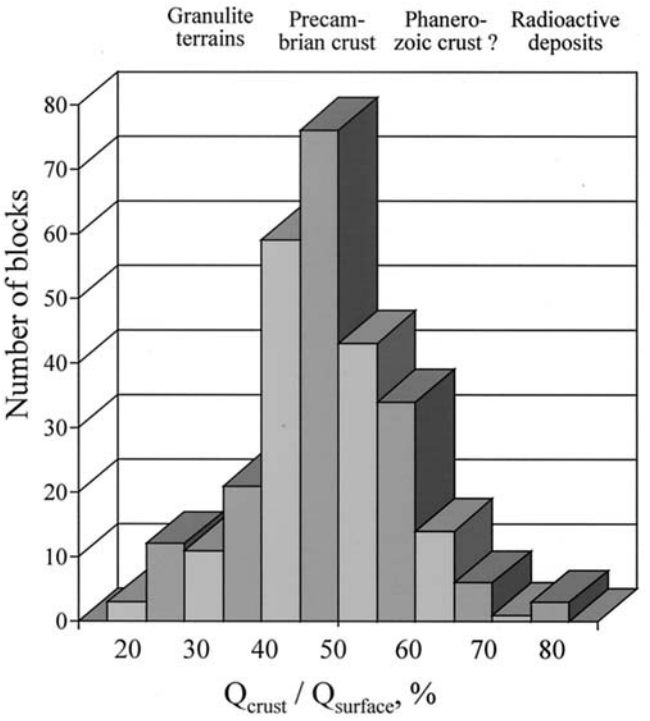

Figure 9. Histogram of the percent of surface heat flow contributed by crustal heat production. The percent contribution for typical Precambrian crust is 40–50%, and increases to 50–60% for Phanerozoic crust. The crust in regions with industrial radioactive deposits contributes 65–80% to the surface heat flow, whereas regions dominated by granulites contribute <35%.

Figure 9 shows the contribution of the crustal heat flow to surface values, as calculated for each of the 300 modeled blocks. Low values of the total crustal heat flow (20–35%) correspond to granulite terranes, whereas large values (65–80%) mainly characterize the regions of industrial radioactive deposits. Figure 10 illustrates the relationship between the surface, reduced, crustal, and mantle heat flow. Heat production in Precambrian crust typically contributes 38–65% of the total measured heat flow, with the combined middle and lower crust contributing ~10–25% and the upper crustal D layer contributing ~30–40% of the total heat flow.

2.4.6. Exposed cross sections of Precambrian upper and middle crust. Measurements of heat production in exposed sections (upper 15–30 km; equivalent to 50–75% of the total crustal thickness in these regions) of Precambrian basement were used as reference models of heat production in the upper middle ancient crust. These include the Vredefort structure in South Africa [*Nicolaysen et al*., 1981], the Wawa-Kapuskasing transect in the Central Superior Province [*Ashwal et al*., 1987], the Pikwitonei structure in Canada [*Fountain et al*., 1987], and the Lewisian terrain from Scotland [*Weaver and Tarney*, 1984] and southern Norway [*Pinet and Jaupart*, 1987].

The contribution to surface heat flow from radioactivity in the middle and lower crust was modeled applying the same assumptions to all crustal blocks. In the middle crust (defined by seismic velocities, usually 6.5–7.0 km/s), heat production ranges from 0.2 to 0.4 μW m^{-3}. In the lower crust ($V_p > 7.0$ km s^{-1}; Table 2) we use a heat production of 0.1 μW m^{-3}. The higher heat production value determined for Precambrian granulite terrains (0.4–0.5 μW m^{-3} [*Ashwal et al*., 1987; *Rudnick and Presper*, 1990]) was not assigned to the entire lower crust, as most granulite terrains represent crustal cross sections down to ~25–30 km only, particularly for Archean crustal sections. The Archean and early Proterozoic lower crust originating below 25–30 km is rarely uplifted and exposed for direct study. Moreover, models with high values of heat production throughout the entire lower crust (0.4–0.5 μW m^{-3}) would predict almost zero mantle heat flow in the regions with low surface heat flow (e.g., the Anabar Shield, the Kola-Karelian Province, the Canadian Shield). To avoid this problem, we used globally lower values of heat production in the lower crust (0.1 μW m^{-3} versus 0.4 μW m^{-3}). This lower value is well within the range of possible heat production in the lowermost crust, which can vary from 0.06 to 0.4 μW m^{-3} in mafic granulites [e.g., *Pinet and Jaupart*, 1987; *Rudnick and Fountain*, 1995].

For a typical 13- to 16-km-thick Precambrian lower crust [*Rudnick and Fountain*, 1995] our lower values of radiogenic heat production result in estimates for mantle heat flow that are 4–5 mW m^{-2} higher than the models based on the 0.4 μW m^{-3} value [e.g., *Mareschal et al*., 1999]. An increase in lower crustal heat production from 0.1 to 0.4 μW m^{-3} will increase our estimates of lithospheric thermal thickness by 20–70 km.

2.4.7. Comparison with petrologic models of radiogenic heat production in the crust. The average values of the total heat production in Archean and post-Archean crust estimated in this study (Tables 4a and 4b) were compared with published estimates derived from petrologic models for Precambrian crustal composition that are constrained mainly by crustal xenoliths [*Gao et al*., 1998; *McLennan and Taylor*, 1996; *Taylor*

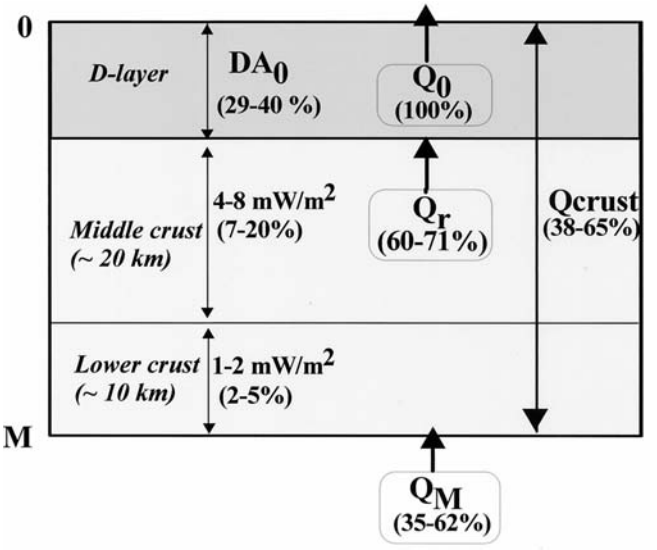

Figure 10. Three crustal layers considered here and their relative contributions to surface heat flow. The radiogenic upper crustal layer is conventionally referred to as the D layer (see Figure 6). This layer contributes 29–40% of the total heat flow (Q_0). The heat flow coming from below the D layer is the reduced heat flow (Q_r) and typically amounts to 60–71% of the total heat flow. Whereas heat production in the entire Precambrian crust typically contributes 38–65% of the total heat flow, the mantle heat flow (Q_M) amounts to 35–62% of the total. These estimates are for a typical Precambrian craton with heat flow in the range 40–55 mW m^{-2} [*Nyblade and Pollack*, 1993].

and McLennan, 1985; *Rudnick and Fountain*, 1995; *Rudnick et al*., 1998; *Shaw et al*., 1986; *Weaver and Tarney*, 1984] (Figure 11). The models of crustal radioactivity used in this study give somewhat lower values for the average crustal heat production in Archean regions (0.29–1.00 μW m^{-3} with typical values of ~0.35–0.55 μW m^{-3}) than estimates by other authors (0.48–0.61 μW m^{-3} [*Rudnick et al*., 1998, and references therein; *Rudnick and Nyblade*, 1999]). For Proterozoic regions our model provides an average crustal heat production of 0.39–1.40 μW m^{-3}, with typical values of ~0.7–0.9 μW m^{-3}, similar to petrologic models that suggest 0.58–1.31 μW m^{-3} as average heat production in the "normal" crust [*Rudnick et al*., 1998]. The main uncertainty for all of these models is the value of heat production ascribed to the lower crust.

2.4.8. Heat production in the upper mantle. A recent study of the composition of the continental lithosphere based on heat flow and xenolith data [*Rudnick et al*., 1998] showed that the concentration of heat-producing elements in cratonic peridotites may not be representative of Archean mantle roots. Thus the choice of heat production values for cratonic lithospheric roots is somewhat arbitrary. In this study the value of heat production for lithospheric mantle was assumed to be 0.01 μW m^{-3} everywhere, which is within the range of the median values of heat production calculated for lithospheric peridotites carried in alkali basalts in Proterozoic continental regions (0.013 μW m^{-3}) and massif peridotites from Phanerozoic fold belts (0.006 μW m^{-3} [*Rudnick et al*., 1998]) and does not contradict other estimates of the mantle heat production (0–0.03 μW m^{-3}) [*Rudnick and Nyblade*, 1999].

2.5. Sensitivity Analysis of Geothermal Modeling

The results of a sensitivity analysis of our geothermal modeling are presented in Table 5. The reference model used in this analysis consists of a 40-km-thick crust with no surficial sediments, surface heat flow in the range 35–60 mW m^{-2}, an average crustal conductivity of 2.7 W m^{-1} K^{-1}, and an upper mantle conductivity of 4.0 W m^{-1} K^{-1}. The average value of radiogenic heat production in the crust was assumed to be 0.44 μW m^{-3} for models with a low surface heat flow (35 mW m^{-2}) and 0.65 μW m^{-3} for models with high heat flow (60 mW m^{-2}), so that the total crustal contribution to the surface heat flow is 40–50% (see Figure 9). Thermal parameters for this reference model were varied to determine the sensitivity of our results to these model parameters.

Table 4a. Average Total Heat Production A in the Archean and Early Proterozoic Crust

Craton	A, μW m^{-3}
Africa	
West Africa	0.36–0.51
Tanzania Craton	0.42–0.56
South Africa	0.49–0.78
South America	
Saõ Francisco Craton	0.31–0.37
Indian Shield	
Dharwar Craton	0.36–0.50
Peninsular Gneiss	0.77
North America	
Superior (Abitibi)	0.34–0.40
Superior (Kapuskasing)	0.29
Entire Superior	0.29–0.47
Greenland	0.52
Australia	
Yilgarn	0.39–0.52
Pilbara	0.56
Kimberly	0.33
Cathaysian Craton	
Sino-Korean Craton	0.57–1.00
Northeastern Europe	
Ukrainian Shield	0.40–0.42
Voronezh Massif	0.36–0.47
Baltic Shield (Kola-Karelia)	0.36–0.49
Siberian Platform	
Anabar Shield	0.17–0.38
Aldan Shield	0.61
Yenisey Ridge	0.20–0.27
Siberian Platform	0.37–0.49

Table 4b. Average Total Heat Production in the Mid-Late Proterozoic Crust

Craton	A, μW m^{-3}
Africa	
Northeastern Africa	0.62–0.64
South Africa	0.61–0.77
South America	
Atlantic Shield	0.62–0.83
Indian Shield	
Gondwana basins	0.86–1.18
North America	
Grenville	0.39–0.95
Australia	
Northern Australia	0.78–1.40
Southern Australia	1.03–1.55
Cathaysian Craton	
Yangtze Craton	0.58–1.24
Northeastern Europe	
Russian Platform	0.83
Siberian Platform	
...	...

The sensitivity analysis shows that the geothermal modeling is relatively insensitive to variations of the crustal or mantle conductivity (Table 5). For example, a reduction of the upper mantle conductivity from 4.0 to 3.3 W m^{-1} K^{-1} leads to a much smaller effect (2–8%) on the estimated geotherms than do variations in heat production in the crust. The sensitivity analysis shows that if the assumed heat production in the crust is increased by 20%, the calculated temperatures at 50 km and 100 km depths would be 9–16% lower and the calculated thickness of the lithosphere (i.e., depth to the 1300°C isotherm) would be 15–30% greater. This makes intuitive sense: For a fixed surface heat flow, higher crustal heat production requires a lower mantle heat flux. We also consider the effects of uncertainties in measured heat flow values and find that for 5% greater surface heat flow the temperature at 50 and 100 km would be 7–9% higher, lithospheric thickness would be 10% less, and calculated mantle heat flow would be 2–3% higher.

3. Thermal State of Precambrian Lithosphere

3.1. Geotherms in Precambrian Cratons

The lithospheric temperature for Precambrian cratons and adjacent regions is displayed in map view for depths of 50, 100, and 150 km in Plates 1, 2, and 3, respectively. These maps are derived from the downward continuation of measured heat flow to obtain numerous geotherms, as described in section 2. Unlike previous studies (Table 1), we used consistent model assumptions for all Precambrian cratons, which permits meaningful comparisons. Estimates of the thermal state of the lithosphere in tectonically active regions (such as the North Amer-

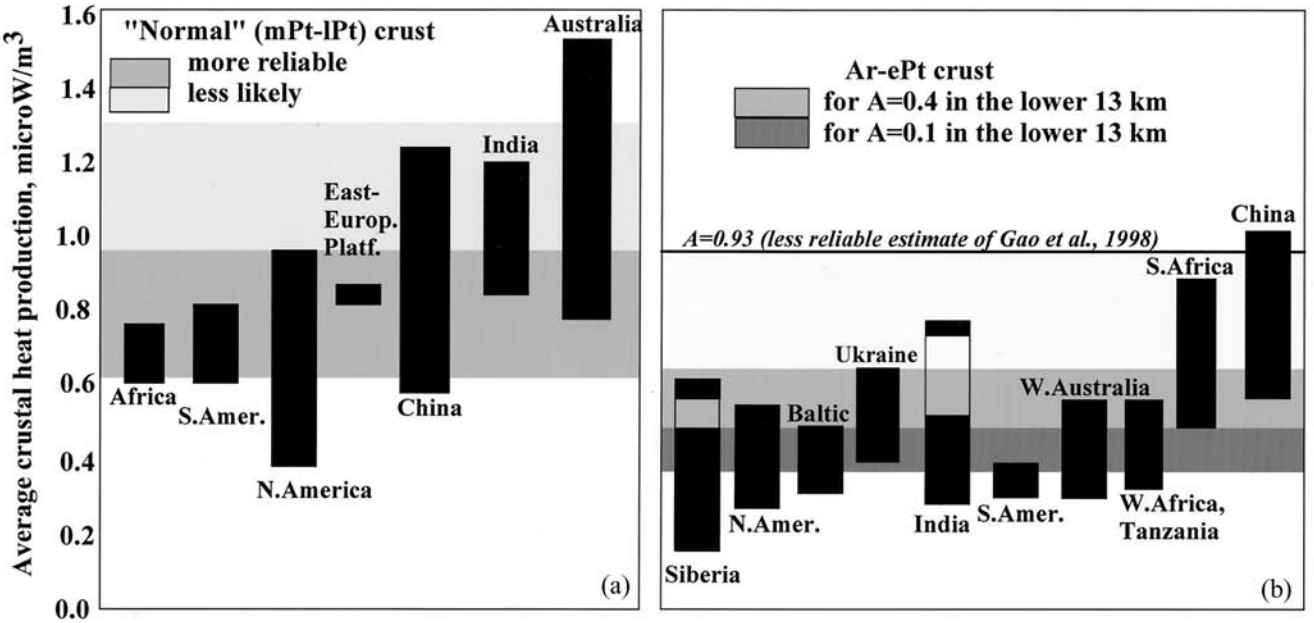

Figure 11. Average range of estimated total crustal heat production in Archean (Ar) and Proterozoic (Pt) crust. Solid bars indicate range of model values used here. Shaded areas are estimates based on petrologic models derived from measurements on xenoliths [*Gao et al*., 1998; *McLennan and Taylor*, 1996; *Taylor and McLennan*, 1985; *Rudnick and Fountain*, 1995; *Rudnick et al*., 1998; *Shaw et al*., 1986; *Weaver and Tarney*, 1984]. (a) Heat production in middle and late Proterozoic regions. (b) Range of heat production for Archean and early Proterozoic crust that generally falls in the range 0.48–0.61 μW m^{-3} if heat production in the lower crust is assumed as $A = 0.4$ μW m^{-3} (light shading). Higher, less common values are in light shading.

ican Cordillera, the Andes, the East African Rift, Tibet, the Himalayas, the Baikal Rift Zone, the Carpathians, and the Caucasus) are not based on our steady state modeling but on petrologic and nonsteady state geothermal constraints available for these regions [e.g., *Decker*, 1995; *Lachenbruch and Sass*, 1977; *Le Pichon et al*., 1997; *Mechie et al*., 1994; *Polyakov et al*., 1988]. In accord with these studies, temperatures at 50 km depth were assumed to be in the range 900–1100°C, and the lithosphere thermal thickness was assumed to be 60–80 km.

Temperatures at 50 km depth (Plate 1) vary widely from ~300°C in cold Archean regions through ~600°C in middle and late Proterozoic blocks to >1000°C in tectonically active regions. Typical temperatures at the Moho were estimated to be 300–500°C in Archean cratons (where the crust is usually ~30–45 km thick but occasionally exceeds 45 km) and 500–800°C in middle and late Proterozoic regions (where crustal thickness is typically 40–55 km and averages ~45 km [*Durrheim and Mooney*, 1994]). Temperatures at 50 km depth beneath Archean cratons (400–600°C; Plate 1) are colder than beneath Proterozoic cratons, confirming a distinction between the deep thermal regime of Precambrian lithosphere of different ages [*Pollack and Chapman*, 1977; *Nyblade*, 1999].

Temperatures at depths of 100 and 150 km (Plates 2 and 3) are lowest beneath the Siberian Platform (including the Anabar Shield) and its margins (the Yenisey Ridge), the Kola-Karelian province of the Baltic Shield, and West Africa. Low temperatures were also estimated for the Tanzanian craton, but the large interpolation step, used to constrain temperature maps, does not permit us to distinguish this cold lithospheric block in Plates 1–3. All of these domains are Archean [*Goodwin*, 1996]. On the whole, we found that the thermal regime of

Table 5. Sensitivity Analysis for the Geothermal Modeling

Change of Model Parameter	Temperature at $z = 50$ km	Temperature at $z = 100$ km	Lithospheric Thickness	Mantle Heat Flow
Average crustal heat production 20% higher	9–13% (50–70°C) lower	11–16% (100–130°C) lower	15–30% (25–80 km) greater	8–10% (4–5 mW m^{-2}) lower
Average crustal conductivity 10% higher	8% (30–60°C) lower	5% (30–60°C) lower	3–6% (5–10 km) greater	the same
Upper mantle conductivity 3.3 W m^{-1} K^{-1} (rather than 4.0 W m^{-1} K^{-1})	2–3% (10–15°C) higher	8% (50–80°C) higher	3–8% (10–15 km) lower	the same
Surface heat flow 5% higher	7–8% (30–50°C) higher	8–9% (50–90°C) higher	10% (10–25 km) lower	2–3% (2–3 mW m^{-2}) higher

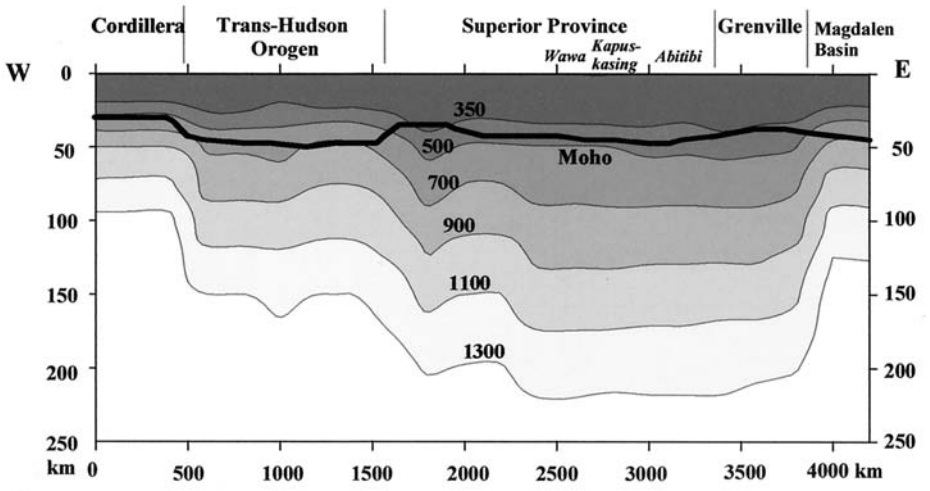

Figure 12. Estimated temperature of the lithosphere of North America along 49°N latitude, passing through the Phanerozoic Cordillera, early Proterozoic Trans-Hudson Orogen, Archean Superior Province, and mid-Proterozoic Grenville Province. Numbers on the curves indicate temperature (in °C). Bold solid line is the base of the crust. Base of the thermal lithosphere is assumed to be the 1300°C isotherm.

the crust and the lithosphere of most of the Archean and early Proterozoic regions is close to the 40 mW m^{-2} geotherm estimated by *Pollack and Chapman* [1977], whereas middle and late Proterozoic blocks are close to their 55 mW m^{-2} geotherm.

The calculated temperature distributions at depths of 100 and 150 km agree well with results from seismic tomography, both globally [e.g., *Nataf and Ricard*, 1996; *Ekström et al*., 1997; *van Heijst and Woodhouse*, 1997] and regionally for Australia [*Van der Hilst et al*., 1998], North America [*van der Lee and Nolet*, 1997], Eurasia [*Ritzwoller and Levshin*, 1998], and Africa [*Ritsema and van Heijst*, 2000]. The thermal and seismic results are in particularly good agreement for Australia where data quality is very good. The agreement for West Africa is very encouraging in view of the fact that the heat flow data are sparse there. Both the seismic and thermal estimates indicate that the Sino-Korean Craton is underlain by warm mantle and lacks a lithospheric root.

Figure 12 shows a cross section of isotherms across the North American lithosphere at 49°N latitude. In accord with the recent results of *Mareschal et al*. [2000a], we find a similar temperature distribution beneath the Superior and Grenville Provinces and an estimated lithospheric thermal thickness of ~200–220 km. However, a comparison of Grenville geotherms with geotherms estimated for other mid-late Proterozoic regions of the world suggests that the Grenville Province is nonrepresentative of crust of this age. Moho temperatures can change significantly over short distances (e.g., from 700°C to ~350°C at the western edge of the Superior Province, Figure 12), mainly reflecting variations in the crustal thickness and composition. The horizontal temperature gradient at the margins of the Precambrian cratons at a depth of ~150–200 km is usually only ~1–2°C km^{-1}. In some active regions it may be an order of magnitude higher and produce the thermomechanical stresses that could result in rifting (e.g., Baikal Rift).

3.2. Sublithospheric Mantle Heat Flow

The estimated values of heat flow at the base of the lithosphere (Q_m) are shown in Plate 4. We note that in contrast to some previous studies, we used a low value for lower crustal radiogenic heat production (0.1 μW m^{-3} versus 0.4 μW m^{-3}). For this reason, our estimates of sublithospheric mantle heat flow are ~4–5 mW m^{-2} higher than estimated by others [e.g., *Mareschal et al*., 2000b; *Jaupart and Mareschal*, 1999].

We found that sublithospheric mantle heat flow beneath Precambrian cratons, calculated here, varies from 10 to 35 mW m^{-2}. The lowest values (Q_m ~ 10 to 15 mW m^{-2}) were estimated beneath the Siberian Platform, West African Craton, and portions of the Baltic Shield. Typical values of Q_m for the Archean lithosphere are 15–25 mW m^{-2} (i.e., Yilgarn, Kaapvaal, and Zimbabwe Cratons; Superior Province; Belo Horizonte block of the Saõ Francisco craton; most of the East European Platform, including the most of the Baltic Shield and Ukrainian Shield; and southern parts of the Indian Shield). Recent studies based on xenolith thermobarometry [*Rudnick and Nyblade*, 1999] suggest that the best estimated values of the heat flow at the base of the lithosphere in the Kaapvaal craton are 14–19 mW m^{-2}, which coincide with the range of values determined in this study. Xenolith data [*Rudnick and Nyblade*, 1999] indicate that mantle heat flow values should be similar beneath the Kaapvaal and Superior Province of the Canadian Shield. This is in accord with our results (18–19 mW m^{-2} for both regions) but differs from those of *Jaupart and Mareschal* [1999], who find a 4 mW m^{-2} difference between these two regions, the Canadian Shield having the lower value.

Sublithospheric mantle heat flow beneath mid-late Proterozoic blocks is typically ~25–35 mW m^{-2}. An exception is the Grenville Province, where Q_m values are similar to the adjacent Archean Superior Province (~18 mW m^{-2}). One explanation may be the fact that the western portion of the Grenville Province is thrust over the lithosphere of the Archean Superior Province [*Ludden*, 1995; *Clowes et al*., 1998], and thus the deep thermal regime of the Grenville Province would be similar to the Superior Province. Taking into account the model differences in radiogenic heat production of the lower crust, our mantle heat flow estimates for the Superior and Grenville Provinces are in close agreement with the recent results of *Mareschal et al*. [2000a].

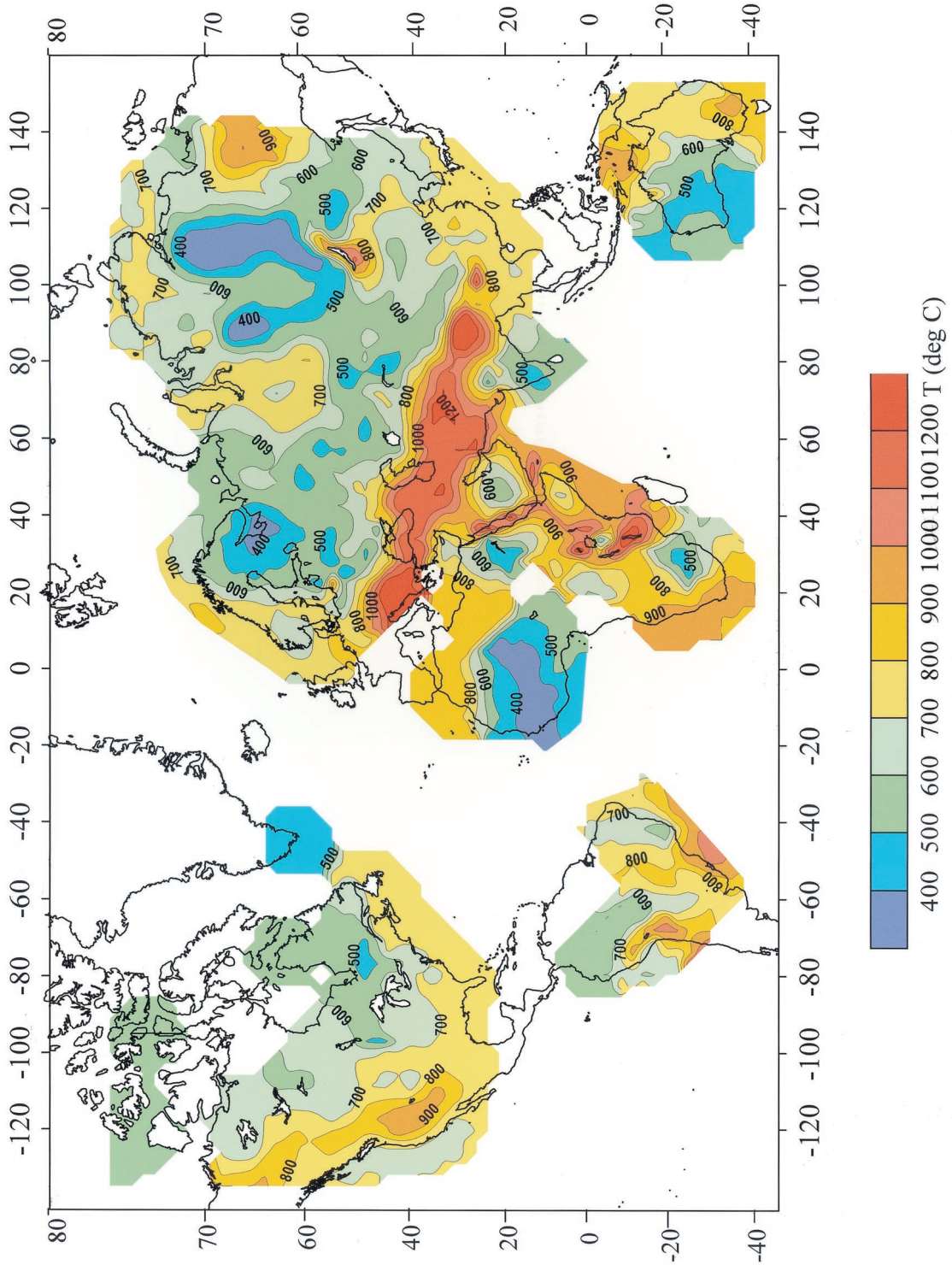

Plate 1. Estimated temperatures at 50 km depth (10° × 10° kriging interpolation), with nonsteady state estimates in noncratonic regions (see text). The range in temperature is 900°C, with the coldest regions corresponding to Archean cratons.

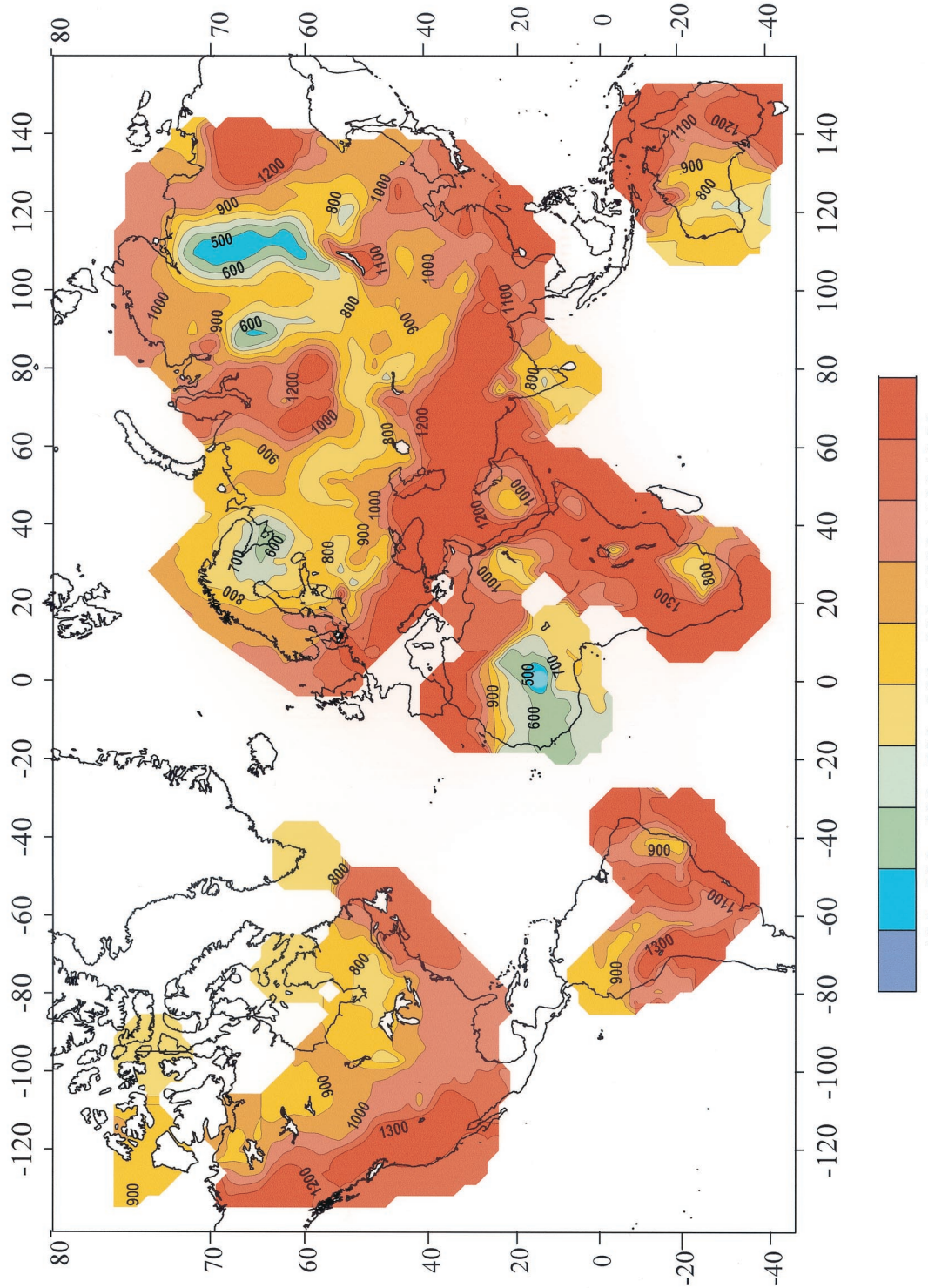

Plate 2. Estimated temperatures at 100 km depth ($10° \times 10°$ kriging interpolation). The range in temperature is at least 600°C (from 700°C to 1300°C) and may be 800°C if the minimum temperature of 500°C is accurate.

3.3. Lithospheric Thermal Thickness

3.3.1. Maps of thickness of the thermal lithosphere. The thickness of the thermal lithosphere, here defined as a conductive layer above a mantle adiabat of 1300°C, was calculated for all of the Precambrian cratons (Plate 5). However, as mantle convection depends on viscosity, which is itself temperature-dependent, the base of the thermal lithosphere is sometimes defined as 0.85 times the solidus temperature (i.e., 1100°C for a mantle solidus of 1300°C), where solid-state creep and associated convective heat transfer are expected to dominate over conduction [e.g., *Pollack and Chapman*, 1977]. Table 6 summarizes the lithosphere's thermal thickness for different Precambrian cratons as estimated in previous studies and this study, for different assumptions for temperatures at the base of the lithosphere. We also compare the results of this study with the only previous global map of lithospheric thermal thickness [*Pollack and Chapman*, 1977], which was calculated from degree-12, spherical harmonic representation of global surface heat flow (Table 6). *Pollack and Chapman* [1977] use the 1130°C isotherm to define the bottom of their thermal lithosphere and find thicknesses >300 km beneath cratonic North America, South America, West Africa, East Siberia, and Western Australia. They report a value of 150–200 km for eastern China and 100–120 km for the Baltic Shield, India, and southern Africa.

We find a typical thermal thickness of Archean lithosphere to be ~200–220 km (most of the East European Platform, South Africa, Western Australia, southern India, the Canadian Shield). However, the thermal thickness of some of the Archean cratons is estimated to be significantly greater than 200 km. The highest values of lithospheric thickness (~300 km and locally even 350 km) were estimated for the West African Craton, the Archean blocks of the Siberian Platform (the Anabar Shield and the Yenisey Ridge), and the Kola-Karelian province of the Baltic Shield. In all of these regions, very low surface heat flows were measured (<30 mW m^{-2} and in some cases as low as 18–25 mW m^{-2}). It is important that for the Siberian Craton (where the surface heat flow does not exceed 25 mW m^{-2} over a large area) our assumed values of the average crustal heat production are much less than usually accepted for the Precambrian crust (Figure 9). Thus our results give a conservative (i.e., lower) estimate of lithospheric thermal thickness for this craton. Heat flow data from West Africa appear to be reliable (J. Behrendt, personal communication, 2000) but are sparse, so thermal modeling there is much less well constrained than for other cratons. However, as noted above, seismic tomography also indicates thick lithosphere in West Africa [*Ritsema and van Heijst*, 2000] (Table 6).

The thinnest Archean lithosphere occurs in South America (170–200 km in the Belo-Horizonte province of the Saõ Francisco Craton in Brazil). However, only small fragments of Archean crust (surrounded by pericratonic mid-Proterozoic mobile belts) have survived in the Saõ Francisco craton, and no heat flow data are available for the adjacent Archean Amazonian and Patagonian cratons. Relatively low values of lithosphere thermal thickness were estimated as well for the Sino-Korean and Yangtze blocks of the Cathaysian Craton, which has been tectonically reworked from the Proterozoic to the present [*Menzies et al*., 1993]. The wide range of lithospheric thermal thicknesses for Archean regions (from 160 to 350 km), which is not observed for regions of any other age, is supported by global seismic tomography studies that show the base of the high-velocity zone (also referred to as the mantle lid or tectosphere) can vary from 100 to 400 km [*Zhang and Tanimoto*, 1993; *Grand*, 1994; *Ekström et al*., 1997; *Polet and Anderson*, 1995].

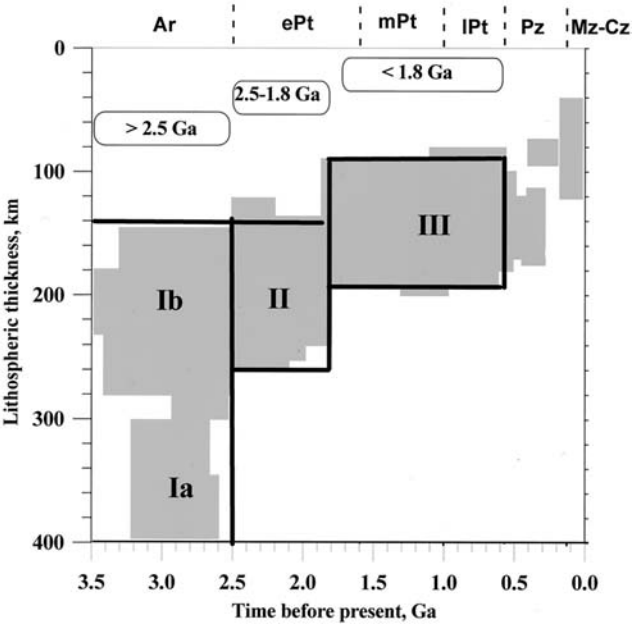

Figure 13. Lithospheric thermal thickness versus geologic age and three stages of formation of the continental lithosphere. The three stages are numbered I through III. Stage I, in the Archean, is divided into two parts, corresponding to the creation of thick lithosphere (>300 km, Ia) and thinner lithosphere (~210 km, Ib) as discussed in the text. Shaded area shows the results of the present geothermal modeling (Plate 5 and Table 6). Ar, Archean; ePt, mPt, lPt, early, middle, and late Proterozoic, respectively; Pz, Paleozoic; Mz-Cz, Meso-Cenozoic.

Compared to Archean lithosphere, the thickness of middle and late Proterozoic lithosphere appears to be more uniform. The calculated thickness ranges from 110–130 km (the Sino-Korean Craton, northern Australia, and the mobile belts around the Kaapvaal and Zimbabwe Cratons) to 150–170 km in mid-Proterozoic blocks of the Baltic and Indian Shields and in Western Australia. Exceptionally thick (≥200 km) Proterozoic lithosphere, similar to that of typical Archean lithosphere, was found only for the Grenville Province and the Trans-Hudson Orogen of the Canadian Shield.

3.3.2. Lithospheric thermal thickness versus age. Figure 13 shows variations of lithospheric thermal thickness with age. We plotted all 300 estimates of lithospheric thermal thickness as rectangles, where the horizontal size gives the range in age [*Goodwin*, 1996], and the vertical size indicates the scatter in estimated lithospheric thickness which results from variations in crustal structure and hence deep thermal properties. The values of the lithosphere thickness were not calculated for Mesozoic and Cenozoic regions; instead, estimates from other studies were used.

The results of thermal modeling show a clear global trend in a progressive thinning of the continental lithosphere with age from 250 ± 70 km in the Archean lithosphere to 200 ± 50 km in early Proterozoic and to ~140 ± 40 km in mid-late Proterozoic lithosphere (Figure 13). Even regions with a somewhat atypical lithospheric thickness (like the Grenville Province) fit

the global trend. However, it is important to note the large scatter in lithospheric thickness (~100 km) for all ages.

It is evident that there are two typical thicknesses of the Archean lithosphere, one ~200–220 km (Figure 13, stage Ib) and the other ~350 km (Figure 13, stage Ia). This result is supported by mantle convection models that suggest the existence of two equilibrium thicknesses of the thermal boundary layer above the convecting mantle: 220 and 350 km [*Doin et al*., 1997]. Isostasy requires that cold, thick lithosphere be chemically depleted [*Jordon*, 1975; *Boyd*, 1989]. Numerical studies indicate that such thick (~350 km) depleted roots can be preserved through geologic time because small-scale mantle convection will primarily affect their horizontal, not vertical, dimension [*Doin et al*., 1997].

The first group of Archean cratons with relatively thin lithospheric roots includes South Africa, Western Australia, the Indian Shield, Cathaysian Craton, and the Saõ Francisco Craton in South America. It is possible that the Congo and Antarctic Cratons, which were adjacent to the above cratons during the existence of the ancient supercontinents (e.g., Rodinia or older), belong to this group as well. The second group of cratons with lithospheric roots exceeding 300 km includes the Siberian Platform, West Africa, and the Baltic Shield. A lack of heat flow data does not permit us to draw any conclusions for some portions of the central and especially northern Canadian Shield (Figure 4), nor for the Amazon Craton, where heat flow data are entirely absent. However, seismic tomography data [e.g., *Polet and Anderson*, 1995] provide strong evidence that the Canadian Shield belongs to the group of Archean cratons with thick lithospheric roots. A recent comparative study of Precambrian South Africa and the Canadian Shield [*Jaupart and Mareschal*, 1999] also supports the idea that these two regions have different deep thermal regimes.

We note that on the basis of lithospheric thickness a subdivision of the Archean–early Proterozoic cratons into two groups seems to have a geographical pattern: cratons in the Southern Hemisphere all have thin lithosphere, whereas cratons in the Northern Hemisphere all have thick lithosphere roots. Such a geographical distribution of lithospheric thickness may reflect the paleogeography of Archean supercontinents or of superplumes that eroded the lithospheric roots in the present-day Southern Hemisphere.

3.3.3. Comparison with other data. The estimates of the lithosphere thermal thickness were compared with geotherms derived from xenolith pressure (P)/temperature (T) data [e.g., *Boyd et al*., 1985; *Boyd and Gurney*, 1986; *O'Reilly and Griffin*, 1985; *Griffin et al*., 1987; *Mackenzie and Canil*, 1997; *Pokhilenko et al*., 1993; *Rudnick and Nyblade*, 1999; *Kukkonen and Peltonen*, 1999; *Kopylova et al*., 1999]. Though we believe that geotherms calculated from P-T data from mantle xenoliths may reflect anomalous, high-temperature geotherms associated with kimberlite volcanism but not the steady state thermal regime of cratonic lithosphere as usually assumed [*O'Reilly and Griffin*, 1985; *Rudnick et al*., 1998; *Rudnick and Nyblade*, 1999; *Russell and Kopylova*, 1999], we compare our results with those derived from the study of xenoliths because such studies provide one of the few independent estimates of lithospheric thermal structure. Good agreement is found for the Kaapvaal Craton and the Proterozoic mobile belts in South Africa, the Baltic Shield, and the Paleozoic terranes of eastern Australia (Table 6). A comparison of xenolith data from the Canadian Shield with geothermal estimates is not possible with the available heat flow measurements from the interior parts of the shield. However, recent xenolith studies for the Slave Province of the Canadian Shield [*Kopylova et al*., 1999] suggest that the lithosphere there was 180–220 km thick at the time of the eruption of these xenoliths. Similar estimates of lithospheric thermal thickness were obtained for the Slave Province in the present study (Plate 5), though only two heat flow measurements exist for this area.

A large discrepancy between the estimates of lithospheric thermal thickness based on geothermal modeling and xenolith P-T data was found for the oldest parts of the Siberian Platform (Table 6). The geothermal models are based on heat flow data from high-quality boreholes where the typical depth is >2 km. We note that the maximum depth for lithospheric kimberlite magmatism rarely exceeds 180–220 km. Therefore xenolith P-T data may not reflect ambient P-T conditions beneath the Archean cratons but rather nonconductive paleogeotherms reflecting the time of kimberlite eruption. Thus these data may give a lower limit on the thickness of the Archean lithosphere (Figure 14a).

Data on the lithospheric thermal thickness were compared with recent global seismic tomography results [*Zhang and Tanimoto*, 1993; *Grand*, 1994; *Polet and Anderson*, 1995; *Ekström et al*., 1997] (Figure 14b). A comparison with some studies is given in Table 6, where the base of the seismic lithosphere corresponds to the depth where the S wave velocity anomaly decreases to less than $+0.5\%$. This comparison supports our finding of thick lithospheric keels (300 km and more) and more beneath the West African and Siberian Cratons and parts of the Baltic Shield. However, the estimates from seismic tomography also indicate thick lithosphere beneath the Kaapvaal Craton and Canadian Shield, a finding not duplicated in our geothermal modeling. However (Figure 4), there is a lack of heat flow data for the core of the Canadian Shield. Seismic data indicate one of the thickest lithospheric roots beneath the Baltic Shield (Table 6). The source of the discrepancy between the geothermal and tomographic results for the Baltic Shield is not clear. Good agreement exists between the geothermal and seismic results for the Western Australian, South American, South African (Kaapvaal), and Cathaysian cratons (Table 6), where both methods show lithospheric roots with a thickness of 150–250 km.

4. Discussion

4.1. Analysis of Heat Production Data

The relationship between heat flow and heat production for Archean and Proterozoic cratons reveals that the radiogenic layer in Archean crust is, on average, much thinner than that of Proterozoic crust. We infer that Archean crust and the post-Archean crust differ in composition. This finding is supported by petrologic studies [*Rudnick et al*., 1998] that show a concentration of heat-producing elements ~3 times higher in xenoliths from Archean than from post-Archean cratons, implying a different composition of the mantle beneath them. The occurrence of diamonds with ages >2.5 Ga indicate that the lithospheric mantle beneath Archean crust is also Archean in age [*Richardson et al*., 1993]. That the crust and mantle beneath Archean cratons are different in composition from that beneath Proterozoic cratons is supported by geochemical studies [*Taylor and McLennan*, 1985; *Boyd*, 1989; *Martin*, 1993, 1994; *Pearson et al*., 1995].

Variations in the depth distribution of radiogenic sources in the crust (as measured by the parameter D in equation (3))

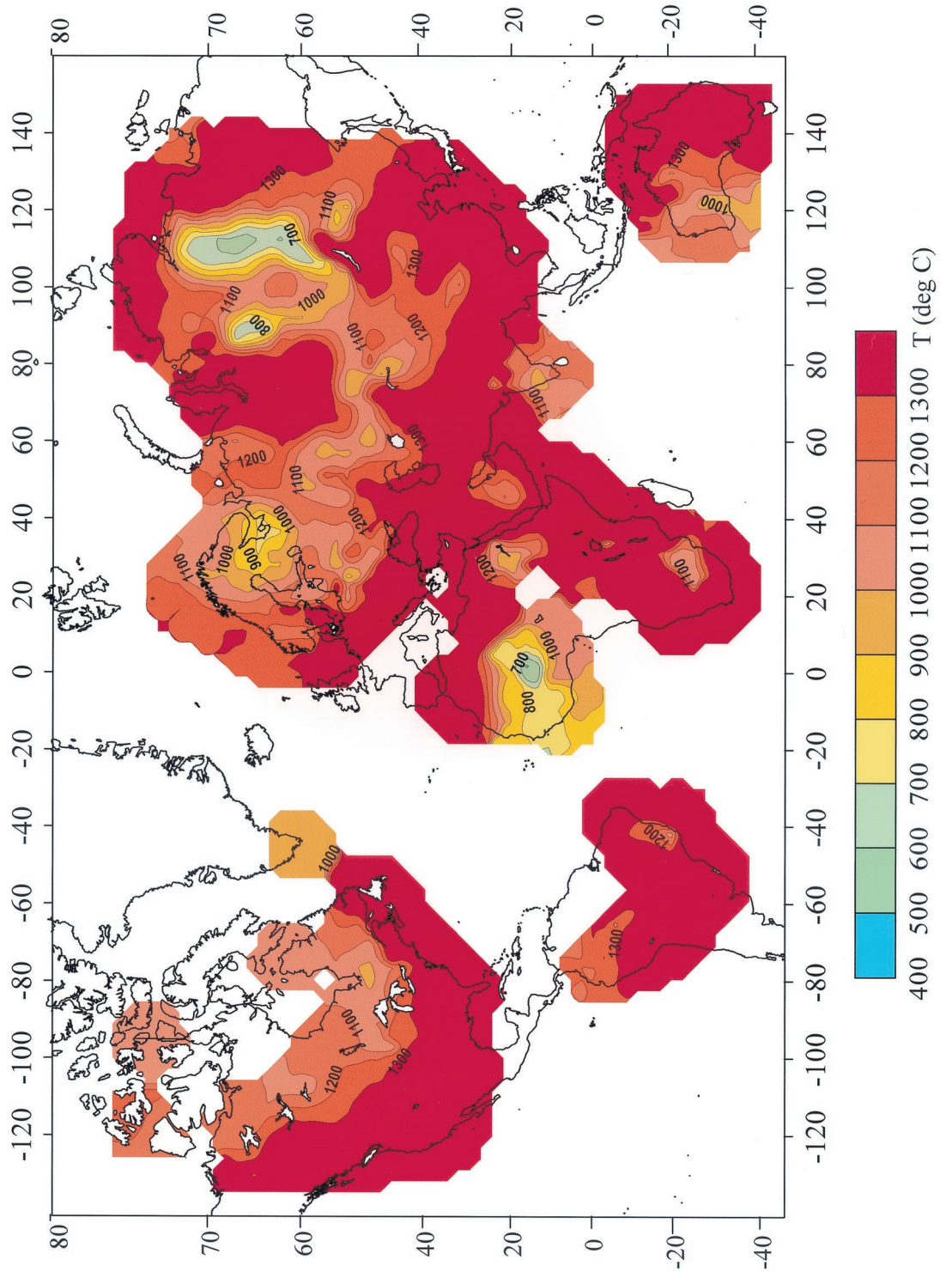

Plate 3. Estimated temperatures at 150 km depth ($10° \times 10°$ kriging interpolation). The range in temperature for most of the map is 400°C (900–1300°C) and may be as large as 600°C considering West Africa and Siberia.

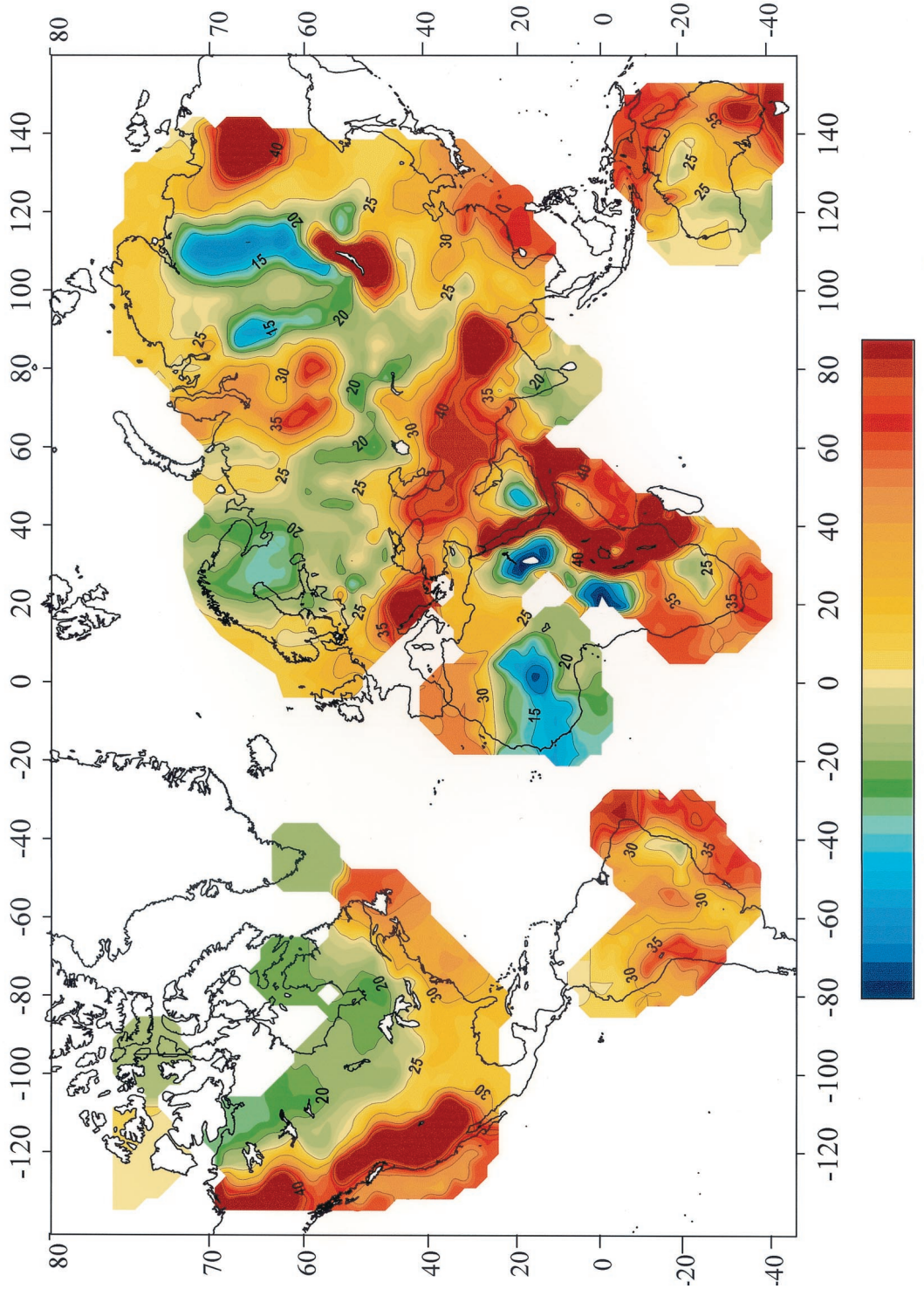

Plate 4. Sublithospheric mantle heat flow ($10° \times 10°$ kriging interpolation). Regions of active tectonism corresponding to nonsteady state heat flow are excluded from the present calculations and were arbitrarily assigned a value of $Q_m = 50$ mW m^{-2} to produce the map.

Table 6. Thickness of the Precambrian Lithosphere

Region	Age	Lithospheric Thermal Thickness From This Study, km		Lithospheric Thermal Thickness Estimated in Previous Studies, km			Depth of Lithospheric Roots From Global Seismic Tomography (+0.5% ΔV), km		Depth of Lithospheric Roots From Regional Seismic Tomography (+1% ΔV),[a] km
		1100°C	1300°C	1100°C	1300°C	Xenolith Data	*Grand* [1994]	*Zhang and Tanimoto* [1993]	
Africa									
West Africa	Ar-ePt	200–280	250–350	>300 [32]	400 [10]	···	450	300	300–400 [33]
Kaapvaal Craton	Ar	150–170	190–210	160 [1], 125–150 [32]	225–250 [21], 200 [1]	>260? [28], 170–190 [4, 5]; 200–250 [34]	···	300	~250 [33]
Tanzanian Craton	Ar	140–160	180–200	···	···	>140 [11]	···	···	250–350 [33]
Damara and Namaqua belts	lPt	80–110	100–140	···	~100 [1]	140 [4, 5]	···	···	···
Australia									
Western Australia	Ar-ePt	140–180	170–230	150 [32]	···	···	···	250	200–300 [36]
Southeastern Australia	lPt-Pz	90–100	110–125	80–100 [16]	···	···	···	···	···
Eastern Australia	Pz-Cz	60–80	80–100	···	···	50–70 [12, 17, 29]	···	···	<80 [36]
Cathaysian Craton									
Tibet median massifs	Ar-mPt	120–150	150–175	100 [32]	130–170 [37]	···	···	···	···
Yangtze Craton	Ar-Cz	90–160	110–200	150 [32]	110–200 [37]	···	···	150	···
Panxi Paleorift	lPt	60–70	70–90	···	75–95 [37]	···	···	···	···
Sino-Korean Craton	Ar-Cz	90–110	120–150	125 [32]	110–140 [37]	···	···	···	···
Indian Shield									
Deccan Plateau	Ar-Pz	120–150	180–200	100–120 [27]	···	···	···	···	···
Dharwar Craton	Ar	160–180	>200	~200 [19], 120–180 [27], 75–100 [32]	···	···	···	100	···
Bastar-Bhandara Craton	ePt-mPt	140–160	170–200	50–60 [27]	···	···	···	···	···
Narmada-Son Basins	Pz-Mz	90–110	120–140	60–80 [27]	···	···	···	···	···
East European Platform									
Lapland and Kola-Karelian Provinces	Ar	180–220	200–300	170–190 [2], >200 [8, 30], 140–180 [9]. 100 [32]	···	>240 [23]	450	400	···
Sveco-Fennian and Transscandinavian	ePt	110–160	110–200	100–160 [2], 120–160 [9]	···	···	···	···	···
Ukrainian Shield	Ar-ePt	140–180	180–230	160–>200 [7], >200 [8], >150 [24]	···	···	···		
Russian Platform	Ar-ePt	130–170	160–220	125–>200 [8] 125–200 [32]	···	···	···	···	···
Siberian Platform									
Interior of Siberian Platform	Ar-ePt	150–300	200–350	>200 [8, 13], >300 [32]	··· ···	~200 [6, 31], >200–250 [34]	···	350	···
Marginal parts of Siberian Platform	mPt-Pz	120–150	140–180	150–200 [8], 200 [32]		···	···	···	···

North American Craton										
Canadian Shield, marginal parts	Ar-ePt	130–200	180–250	200 [32]	200–290 [20,26]	>200–250 [34]	…	…	…	…
Canadian Shield, north central parts	Ar-ePt	…	…	>300 [32]	…	…	350	350	…	…
Slave Province	Ar	…	…	…	…	180–220 [18, 22, 25] >200–250 [34]	…	…	…	…
Somerset Island	ePt	140–170	160–200	100–200 [32]		140 [35]	…	…	…	…
Wyoming	Ar	110–120	140–150	…	>150 [3], >170 [14]	>170 [15]	…	…	…	…
Grenville Prov.	mPt	120–150	150–200	150 [32]	…	…	…	…	…	…
Appalachians	Pz	90–120	110–150	100–150 [32]	…	…	…	…	…	…
South American Craton										
Amazonian Craton	Ar-ePt	…	…	300 [32]	…	…	200	200	…	…
São Francisco Craton	Ar-ePt	130–160	170–200	300 [32]	…	…	…	…	…	…

[a]Bracketed numbers indicate references as follows: 1, *Ballard and Pollack* [1987]; 2, *Balling* [1995]; 3, *Blackwell* [1991]; 4, *Boyd and Gurney* [1986]; 5, *Boyd et al.* [1985]; 6, *Boyd et al.* [1995]; 7, *Burianov et al.* [1985]; 8, *Cermak* [1982]; 9, *Cermak and Bodri* [1995]; 10, *Chapman and Pollack* [1974]; 11, *Chesley et al.* [1999]; 12, *Cull et al.* [1991]; 13, *Duchkov et al.* [1987]; 14, *Eggler et al.* [1988]; 15, *Eggler* [1987]; 16, *Ferguson et al.* [1979]; 17, *Griffin et al.* [1987]; 18, *Griffin et al.* [1999]; 19, *Gupta et al.* [1991]; 20, *Jaupart et al.* [1998]; 21, *Jones* [1988]; 22, *Kopylova et al.* [1999]; 23, *Kukkonen and Peltonen* [1999]; 24, *Kutas et al.* [1989]; 25, *MacKenzie and Canil* [1997]; 26, *Mareschal et al.* [2000a]; 27, *Negi et al.* [1986, 1987]; 28, *Nicolaysen et al.* [1981]; 29, *O'Reilly and Griffin* [1985]; 30, *Pasqualle et al.* [1991]; 31, *Pokhilenko et al.* [1993]; 32, *Pollack and Chapman* [1977]; 33, *Ritsema and van Heijst* [2000]; 34, *Rudnick and Nyblade* [1999]; 35, *Schmidberger and Francis* [1999]; 36, *Simons et al.* [1999]; 37, *Wang* [1996].

with age show a different pattern for the cratons of the Northern and Southern Hemispheres. For the Southern Hemisphere cratons (South Africa, Western Australia, South America), D increases from 2–5 km in Archean crust to 6–10 km in late Proterozoic crust. However, this trend does not exist for the Northern Hemisphere cratons. D values for the Archean–early Proterozoic blocks of North America and Eurasia show a large unsystematic scatter from 5 to 17 km. Estimates for the West African Craton are similar to those from the Archean Canadian Shield and Eurasia. However, in mid-late Proterozoic crust, D values fall into the same range for all cratons (5–11 km). Variations in the depth distribution of crustal radiogenic sources with age may reflect different conditions of the formation of cratons in the Northern and Southern Hemispheres in the Archean and early Proterozoic.

4.2. Density of Lithospheric Roots

Presumably, the Archean lithosphere is in isostatic equilibrium, so different compositions of Northern and Southern Hemisphere cratons may compensate for differences in lithospheric roots, with the cratons in the Northern Hemisphere having a lower mean lithospheric density. Using the temperatures at the base of the crust and typical lithosphere thicknesses from this study, we now estimate the density contrast between the asthenosphere and the lithospheric mantle for northern and southern Archean lithosphere. The calculations follow the approach of *Lachenbruch and Morgan* [1990] and are based on the assumption that isostatic balance is achieved locally at the base of the lithosphere. In this method, the observed elevation is maintained by crustal and mantle lithospheric contributions to buoyancy. Crustal buoyancy is the product of crustal thickness and average crustal density. Mantle lithospheric buoyancy is the product of mantle lithospheric thickness (calculated in this study, Plate 5) and average lithospheric density corrected for thermal expansion using our calculated geotherms. Elevation, crustal density, and crustal thickness are based on CRUST 5.1 [*Mooney et al*., 1998]. Once all these parameters are determined, the remaining free parameter is mantle lithospheric density, which in turn depends on the degree of chemical depletion of the lithosphere.

Our isostatic calculations suggest that all Archean cratons (i.e., in both the Northern and Southern Hemispheres) have a composition that is 1.5% less dense (depleted) than the underlying asthenosphere. This result agrees with estimates derived from xenoliths [*Boyd and McCallister*, 1976; *Boyd*, 1989; *Hawkesworth et al*., 1990] and from theoretical considerations [*O'Hara*, 1975; *Jordan*, 1979, 1988; *Ballard and Pollack*, 1988]. The equality of lithospheric depletion estimated for all Archean and early Proterozoic cratons is a consequence of systematic variations in crustal thickness of the Northern and Southern Hemisphere cratons (36–62 km, with an average of 45 km, and 30–43 km, with an average of 35 km, respectively). Isostatic calculations show that small (5–6 km) variations in crustal thickness may compensate for variations of up to 150 km in the thickness of lithospheric roots.

The equality of the estimated depletion for the lithospheric roots of Archean and early Proterozoic cratons of both Northern and Southern Hemispheres suggests that they formed under similar conditions. However, the systematic difference in the crustal and lithospheric thicknesses between the Archean/early Proterozoic cratons of Northern and Southern Hemispheres suggests either two different mechanisms of their for-

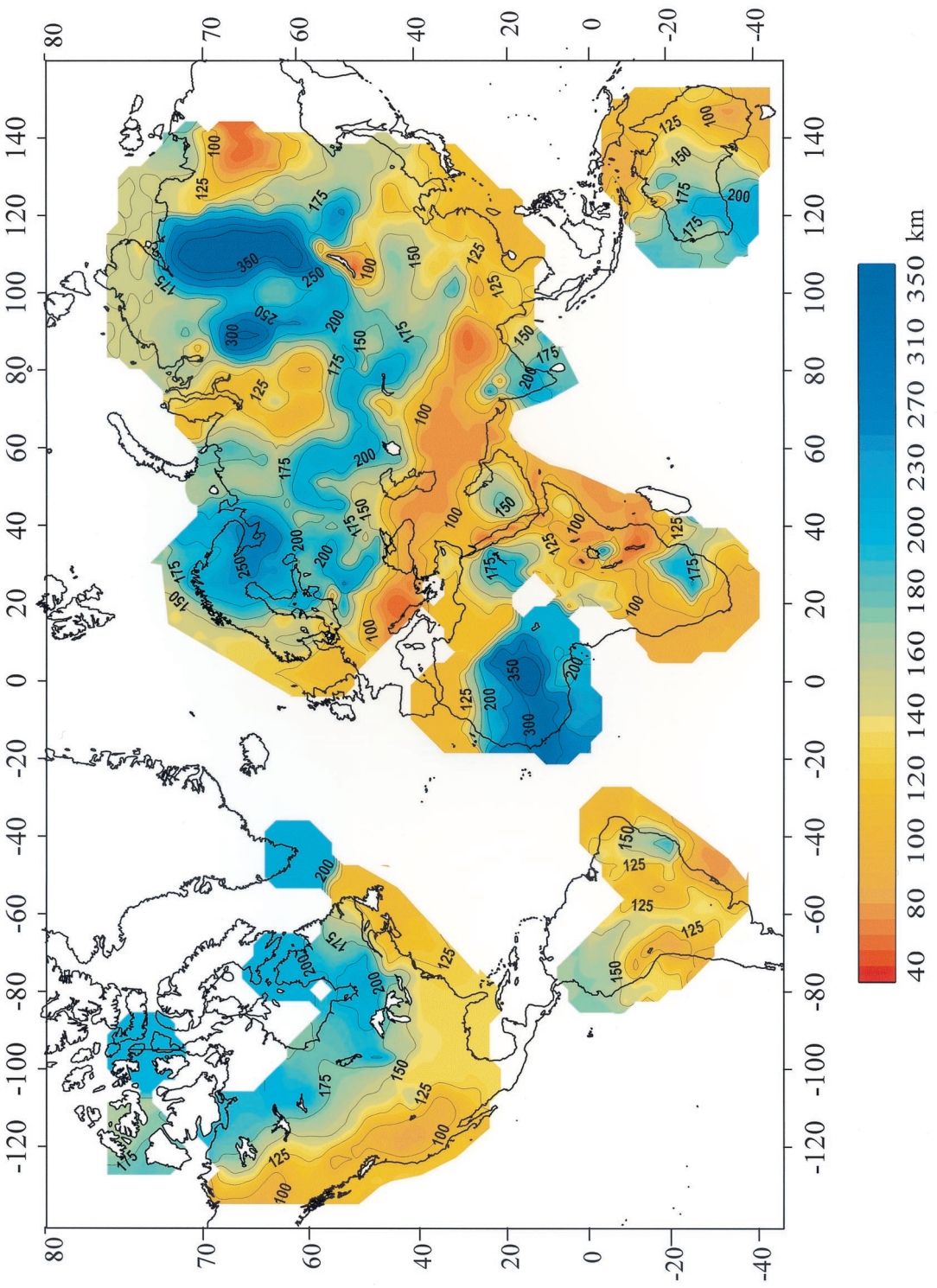

Plate 5. Map of lithospheric thermal thickness, which is assumed to be the depth of the 1300°C adiabat (10° × 10° kriging interpolation). The Precambrian lithosphere ranges in thickness from 140 to 350 km, with the thickest lithosphere beneath West Africa, the Baltic Shield, and Siberia. These results are sorted by crustal age in Figure 13 and are compared with independent estimates based on studies of mantle xenoliths and seismic tomography in Figure 14. Thick lithosphere (>300 km) is found only in the Northern Hemisphere (see text for discussion).

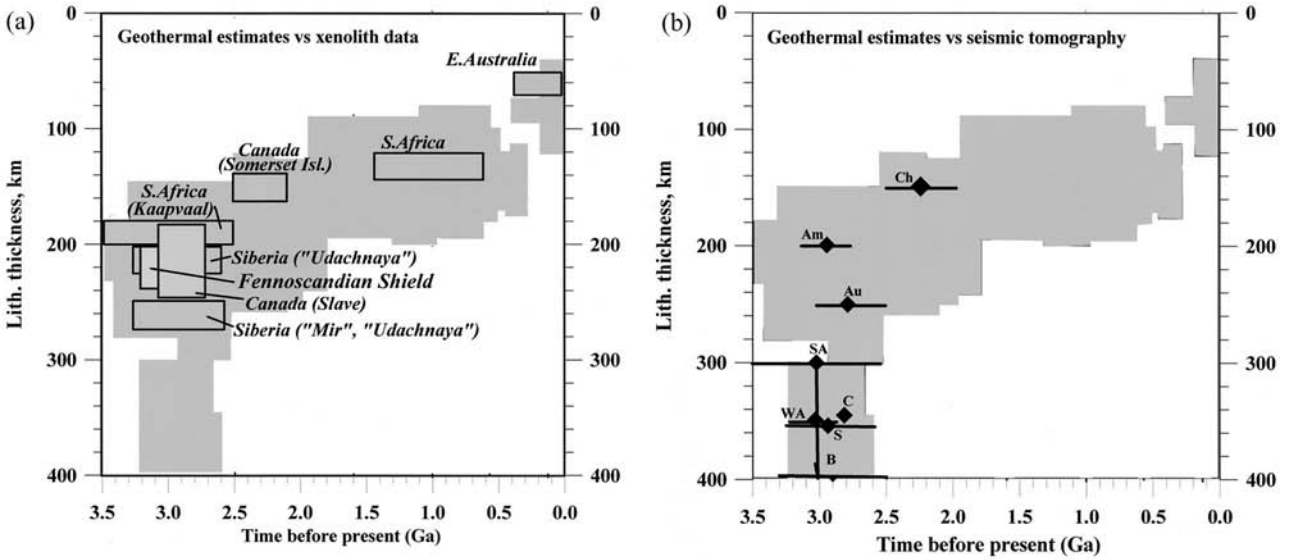

Figure 14. A comparison of thermal lithosphere thickness with (a) xenolith and (b) seismic tomography data. In Figure 14a, the shaded area indicates lithospheric thickness as estimated from the present geothermal modeling (Plate 5 and Table 6). Shaded boxes indicate xenolith data; the horizontal size reflects age variations as given by *Goodwin* [1996]; the vertical size reflects variations and/or errors in depth estimates. Xenolith data are for South Africa from *Boyd et al*. [1985], *Boyd and Gurney* [1986], and *Ryan et al*. [1996]; for the Canadian Shield from *MacKenzie and Canil* [1997], *Rudnick et al*. [1998], *Schmidberger and Francis* [1999], *Kjarsgaard and Peterson* [1992], and *Kopylova et al*. [1999]; for the Siberian Craton from *Boyd et al*. [1985, 1995], *Boyd* [1994], *Griffin et al*. [1993, 1996], *Pokhilenko et al*. [1993], and *Ryan et al*. [1996]; for eastern Australia from *Griffin et al*. [1987] and *O'Reilly and Griffin* [1985]; and for the Baltic Shield from *Kukkonen and Peltonen* [1999]. In Figure 14b, the shaded area indicates lithospheric thickness as estimated from the present geothermal modeling (Plate 5 and Table 6). Diamonds and lines are seismic tomography data from *Grand* [1994] and *Zhang and Tanimoto* [1993] (assuming the base of the lithosphere at the depth where the V_S anomaly decreases below +0.5%). The horizontal length of error bars reflects age variations as given by *Goodwin* [1996], and the vertical length reflects the span given by *Grand* [1994] and *Zhang and Tanimoto* [1993]. Am, Amazonian Craton; Au, Western Australian Craton; B, Baltic Shield; C, Canadian Shield; Ch, Cathaysian Craton; S, Siberian Craton; SA, South African Craton; WA, West African Craton.

mation or distinct tectonic histories for northern versus southern cratons.

We next consider the amount of depletion for middle and late Proterozoic lithosphere, again using the approach of *Lachenbruch and Morgan* [1990]. The difference in crustal thickness between northern and southern cratons disappears for crust younger than ~2.0 Ga. Using our estimates of the thermal thickness of middle and late Proterozoic lithosphere, buoyancy requires that the subcrustal lithosphere should be depleted by ~0.6–0.7% relative to the asthenosphere.

Buoyancy can be achieved by chemical depletion due to the extraction of basaltic constituents [*Jordan*, 1979] or by any magmatic process that will make the mantle composition richer in magnesium than iron [e.g., *Pollack*, 1986]. Indeed, an increased Mg/(Mg + Fe) ratio in the lithospheric mantle beneath all Archean cratons is supported by peridotite xenolith data. In particular, xenolith data give exactly the same Mg/(Mg + Fe) ratio for xenoliths from the Kaapvaal and Siberian Cratons [*Boyd*, 1989; *Boyd et al*., 1993], which agrees with our conclusion that the lithospheric mantle of these cratons have equivalent amounts of chemical depletion.

4.3. Three Stages of Formation of Precambrian Continental Lithosphere

The evolution of continental lithosphere since 4.0 Ga is much debated, with many hypotheses developed from the consequences of a mantle cooling rate estimated between ~50°C/Gyr [*Abbott et al*., 1994] and ~85°C/Gyr [*De Smet et al*., 2000]. Comprehensive reviews of these hypotheses are provided by *Condie* [1997, 1998, 2000], *Davies* [1999], and *De Smet et al*. [2000]. The results presented in Figure 13 allow us to postulate three major stages in the formation of Precambrian continental lithosphere. We assume that the crust and its underlying mantle lithosphere formed at essentially the same time (within 50 to 100 Myr [*Pearson*, 1999]).

1. The first stage occurred in the period 4.0–2.5 Ga, with a pronounced peak in lithospheric formation at 2.7 Ga [*Condie*, 1997, 1998]. We hypothesize that two types of lithosphere were formed during this early stage, characterized by different crustal structure and lithospheric thickness but similar composition (density) of the lithospheric mantle. We speculate that the two types of lithosphere were formed by different processes, one involving lithospheric formation above a high-temperature plume and yielding at least 350-km-thick lithosphere, the other involving lithospheric formation by tectonic stacking of relatively buoyant (compared with present-day) oceanic lithospheric plates subducted at a shallow angle and yielding ~220-km-thick lithosphere.

2. The early Proterozoic (~2.5–1.8 Ga) was a transitional regime: Because of a gradual decrease in mantle temperature the process leading to the formation of a thick lithosphere (>300 km) no longer operated, but the formation of litho-

sphere of intermediate thickness (160–240 km) by subduction of relatively buoyant oceanic plates continued until ~1.8 Ga.

3. Lithosphere younger than ~1.8 Ga never formed with a thickness in excess of 170–180 km. The fact that diamonds are rare in middle and late Proterozoic lithosphere [*Richardson et al*., 1993] provides evidence that the thermal lithosphere (defined here as the depth to the 1300°C adiabat) never exceeded 170–180 km, the depth required for the diamond stability field at $T \sim 1300$°C [*Kennedy and Kennedy*, 1976]. Because of the cooling of the Earth, high-temperature melting conditions, with as much as 30% mantle melt at depths of 400–600 km [*Arndt*, 1994] ceased by the end of Archean time.

These three stages of lithospheric formation, distinguished by geothermal modeling, correlate with geologic data. The transition from the first to the second stage at ~2.5 Ga approximately corresponds to the end of the extraction of komatiites from the mantle, most of which are older than 2.5 Ga [*Arndt*, 1994]. Komatiite extraction was followed by a steady decrease of mantle temperatures [e.g., *Vlaar et al*., 1994] and a secular decrease in depth of melting in mantle plumes [*Herzberg*, 1995]. This temperature decrease as well as change in mantle composition after komatiite extraction may have contributed to the formation of Proterozoic lithospheric roots that are chemically different from Archean roots.

The restricted time intervals for the ages of banded iron formations, greenstone belts, large igneous provinces, and giant dike swarms [e.g., *Condie*, 1997, 1998; *Yale and Carpenter*, 1998; *Nelson*, 1998] suggest that many processes evolve with time and presumably are associated with changes in mantle convection due to cooling of the Earth. For example, from the distribution of crustal ages, *Condie* [1995] distinguished three stages of mantle convection, >2.8 Ga, 2.8–1.3 Ga, and <1.3 Ga, and *Condie* [1997, p. 177] suggests that "from the early Proterozoic onwards, ... crustal and mantle processes would operate much like they do today."

5. Conclusions

1. The steady state thermal conductivity equation was used to estimate temperature distribution and thermal thickness of Precambrian lithosphere. The heat flow data from the global compilation by *Pollack et al*. [1993], augmented by more recent data, provided much of the basis for modeling. The same geothermal constraints were used for all of the Precambrian cratons to permit quantitative comparison of the results. About 500 models of the depth distribution of heat-producing elements (HPEs), used to calculate continental geotherms, were based on laboratory studies of heat production in near-surface rocks, data on seismic velocities in the crust, direct HPE measurements in exposed Precambrian crust, and petrologic constraints on the total crustal heat production.

2. The depth distribution of HPEs was considered as well in the framework of the heat flow provinces. The parameters D (characteristic depth of crustal heat-producing elements) and Q_r (reduced heat flow) were estimated separately for geologic provinces of different tectonothermal age. This analysis revealed that the depth distribution of HPEs differs in Archean and Proterozoic crust. The reduced mantle heat flow shows a secular increase from Archean to late Proterozoic.

The relationship of surface to reduced heat flow proposed by *Pollack and Chapman* [1977] was evaluated separately for Archean/early Proterozoic and middle/late Proterozoic crust. We found that no more than 30% of the observed heat flow in Archean/early Proterozoic regions can be attributed to upper crustal radioactivity, and the typical contribution of the upper crustal D layer into the surface heat flow is ~12 mW m^{-2} for Archean/early Proterozoic crust and 18 mW m^{-2} for middle/late Proterozoic crust.

3. We estimated the temperature distribution in Precambrian lithosphere and produced maps for temperatures at depths of 50, 100, and 150 km. The thermal states of Archean/early Proterozoic and middle/late Proterozoic cratons differ. On average, their respective lithospheric temperature distribution is close to the geotherms estimated by *Pollack and Chapman* [1977] for surface heat flow of 40 and 55 mW m^{-2}, respectively. The estimated temperatures at the base of the Archean/early Proterozoic and middle/late Proterozoic crust are 300–500°C and 500–800°C, respectively.

4. Heat flow from the sublithospheric mantle in the Precambrian cratons varies from ~10 to 35 mW m^{-2}. Typical values in Archean blocks are ~15–25 mW m^{-2}, with very low values (10–15 mW m^{-2}) for the Siberian Platform and West Africa. Sublithospheric mantle heat flow in Proterozoic blocks is typically ~25–35 mW m^{-2}.

5. Lithospheric thermal thickness was calculated as a conductive layer above a mantle adiabat of 1300°C. We found a global trend in a secular thinning of the continental lithosphere from ~250 ± 70 km in Archean lithosphere through 200 ± 40 km in early Proterozoic to 140 ± 40 km in mid-late Proterozoic lithosphere.

6. Archean cratons have two characteristic average lithospheric thicknesses: ~210 km and ~350 km. The cratons with relatively thin lithospheric roots are presently located mainly in the Southern Hemisphere and include South Africa, Western Australia, and South America. Archean cratons of the Northern Hemisphere with a very thick lithosphere include the Baltic Shield, the Siberian Platform, West Africa, and possibly the central and northern Canadian Shield.

7. Buoyancy estimates show that the same degree of lithospheric mantle depletion (1.5%) is required for all Archean/early Proterozoic cratons. Isostatic balance of the lithosphere is achieved by thermal effects and variations in crustal thickness: the thicker lithosphere of the Northern Hemisphere has an average crustal thickness of ~45 km, whereas the thinner lithosphere of the Southern Hemisphere has an average crustal thickness of ~35 km.

8. Analysis of the age dependence of the lithospheric thermal thickness allows us to hypothesize three stages in the formation of the continental lithosphere: >2.5 Ga, 2.5–1.8 Ga, and <1.8 Ga. We relate these three stages to a gradual decrease in mantle temperature that was accompanied by changes in mantle convection patterns [*Condie*, 1998; *Davies*, 1999; *De Smet et al*., 2000]. Support for this hypothesis can be found in restricted ages of greenstone belts, komatiites, banded iron formations, and giant dike swarms. (The results are available from the authors at http://www.geofys.uu.se/~iartem.)

Acknowledgments. Reviews of M. Fowler, C. Jaupart, N. Godfrey, K. Whaler, G. Chulick, G. Clitheroe, G. Thompson, R. Mereu, C. Ebinger, M. Menzies, H. Thybo, and R. Girdler are greatly appreciated. W. B. Hamilton and D. M. Fountain provided extensive comments and suggestions. Discussions with J.-C. Mareschal at the University of Quebec, Montreal; C. Jaupart, A. Hirn, and J. P. Montagner at the Institut Physique du Globe de Paris; and David Gee at the University of Uppsala were very helpful. We are grateful to H. N.

Pollack, S. J. Hurter, and J. R. Johnson for compiling the heat flow data used here. This study was supported in part by the USGS Earthquake Hazards Reduction Program and the U.S. Department of Energy Program NN-20. I.M.A. gratefully acknowledges partial support from De Beers Consolidated Mines in 1997–1998.

References

Abbott, D. H., R. Drury, and W. H. F. Smith, The flat to steep transition in subduction style, *Geology*, *22*, 937–940, 1994.

Anderson, D. L., *Theory of the Earth*, 366 pp., Blackwell, Malden, Mass., 1989.

Anderson, D. L., Superplumes or supercontinents?, *Geology*, *22*, 39–42, 1994.

Anderson, D. L., and C. G. Sammis, Partial melting in the upper mantle, *Phys. Earth Planet. Inter.*, *3*, 41–50, 1970.

Arndt, N. T., Archean komatiites, in *Archean Crustal Evolution*, edited by K. C. Condie, pp. 11–44, Elsevier Sci., New York, 1994.

Arshavskaya, N. I., On the linear relationship between heat flow and heat generation in the shields (in Russian), in *Experimental and Theoretical Studies of Heat Flow*, pp. 177–194, Nauka, Moscow, 1979.

Ashwal, L. D., P. Morgan, S. A. Kelley, and J. A. Percival, Heat production in an Archean crustal profile and implications for heat flow and mobilization of heat-producing elements, *Earth Planet. Sci. Lett.*, *85*, 439–450, 1987.

Ballard, S., and H. N. Pollack, Diversion of heat by Archean cratons: A model for southern Africa, *Earth Planet. Sci. Lett.*, *85*, 253–264, 1987.

Ballard, S., and H. N. Pollack, Modern and ancient geotherms beneath southern Africa, *Earth Planet. Sci. Lett.*, *88*, 132–142, 1988.

Ballard, S., H. N. Pollack, and N. J. Skinner, Terrestrial heat flow in Botswana and Namibia, *J. Geophys. Res.*, *92*, 6291–6300, 1987.

Balling, N., Heat flow and lithospheric temperature along the northern segment of the European Geotraverse, in *Proceedings of the 6th Workshop European Geotraverse (EGT) Project*, edited by R. Freeman and St. Mueller, pp. 405–416, Eur. Sci. Found., Strasbourg, France, 1990.

Balling, N., Heat flow and thermal structure of the lithosphere across the Baltic Shield and northern Tornquist Zone, *Tectonophysics*, *244*, 13–50, 1995.

Baumann, M., and L. Rybach, Temperature field modelling along the northern segment of the European geotraverse and the Danish transition zone, *Tectonophysics*, *194*, 387–408, 1991.

Beck, A. E., Climatically perturbed temperature gradients and their effect on regional and continental heat-flow means, *Tectonophysics*, *41*, 17–39, 1977.

Birch, F., E. R. Roy, and E. R. Decker, Heat flow and thermal history and New England and New York, in *Studies of Appalachian Geology*, edited by E. An-Zen, pp. 437–451, Wiley-Interscience, New York, 1968.

Blackwell, D., Heat-flow patterns of the North American continent: A discussion of the geothermal map of North America, in *Neotectonics of North America*, edited by D. B. Slemmons, pp. 423–436, Geol. Soc. of Am., Boulder, Colo., 1991.

Bodri, B., and A. M. Jessop, Geothermal model of the continental margins of eastern Canada, *Tectonophysics*, *164*, 139–150, 1989.

Boyd, F. R., Siberian geotherm based on lherzolite xenoliths from Udachnaya kimberlite, USSR, *Geology*, *12*, 528–530, 1984.

Boyd, F. R., Compositional distinction between oceanic and cratonic lithosphere, *Earth Planet. Sci. Lett.*, *96*, 15–26, 1989.

Boyd, F. R., and J. J. Gurney, Diamonds and the African lithosphere, *Science*, *232*, 472–477, 1986.

Boyd, F. R., and R. H. McCallister, Densities of fertile and sterile garnet peridotites, *Geophys. Res. Lett.*, *3*, 509–512, 1976.

Boyd, F. R., J. J. Gurney, and S. H. Richardson, Evidence for a 150–200-km thick Archean lithosphere from diamond inclusion thermobarometry, *Nature*, *315*, 387–389, 1985.

Boyd, F. R., D. G. Pearson, N. P. Pokhilenko, and S. A. Mertzman, Cratonic mantle composition: Evidence from Siberian xenoliths, *Eos Trans. AGU*, *74*(16), Spring Meet. Suppl., 321, 1993.

Boyd, F. R., N. P. Pokhilenko, D. G. Pearson, and N. V. Sobolev, Peridotite xenoliths from the Udachnaya kimberlite pipe, paper presented at 6th International Kimberlite Conference, Inst. of Geol. and Geophys., Russ. Acad. of Sci., Novosibirsk, Russia, Aug. 1995.

Burianov, V. B., V. V. Gordienko, O. V. Zavgorodniaya, S. N. Kulik, and I. M. Logvinov, *Geophysical Model of the Tectonosphere of Ukraine* (in Russian), 212 pp., Naukova Dumka, Kiev, Russia, 1985.

Cermak, V., Geothermal model of the lithosphere and the map of the lithosphere thickness for the USSR territory (in Russian), *Izv. Akad. Nauk SSSR Fiz. Zemli*, *11*, 25–38, 1982.

Cermak, V., and L. Bodri, Two-dimensional temperature modelling along five East-European geotraverses, *J. Geodyn.*, *5*, 133–163, 1986.

Cermak, V., and L. Bodri, Three-dimensional deep temperature modelling along the European geotraverse, *Tectonophysics*, *244*, 1–11, 1995.

Cermak, V., and A. M. Jessop, Heat flow, heat generation and crustal temperature in the Kapuskasing area of the Canadian Shield, *Tectonophysics*, *11*, 287–303, 1971.

Cermak, V., and L. Rybach, Thermal conductivity and specific heat of minerals and rocks, in *Landolt-Bornstein Numerical Data and Functional Relationships in Science and Technology*, edited by G. Angenheister, pp. 213–256, Springer-Verlag, New York, 1982.

Cermak, V., J. Safanda, and A. Guterch, Deep temperature distribution along three profiles crossing the Teisseyre-Tornquist tectonic zone in Poland, *Tectonophysics*, *164*, 151–163, 1989.

Chapman, D. S., Thermal gradients in the continental crust, in *The Nature of the Lower Continental Crust*, edited by J. B. Dawson et al., *Geol. Soc. Spec. Publ.*, *24*, 63–70, 1986.

Chapman, D. S., and H. N. Pollack, "Cold spot" in West Africa: Anchoring the African plate, *Nature*, *250*, 477–478, 1974.

Chapman, D. S., and H. N. Pollack, Heat flow and heat production in Zambia: Evidence for lithospheric thinning in central Africa, *Tectonophysics*, *41*, 79–100, 1977.

Chesley, J. T., R. L. Rudnick, and C.-T. Lee, Re-Os systematics of mantle xenoliths from the East African Rift: Age, structure, and history of the Tanzanian craton, *Geochim. Cosmochim. Acta*, *63*, 1203–1217, 1999.

Christensen, N. I., and W. D. Mooney, Seismic velocity structure and composition of the continental crust: A global view, *J. Geophys. Res.*, *100*, 9761–9788, 1995.

Clowes, R. M., F. A. Cook, and J. N. Ludden, Lithoprobe leads to new perspectives on continental evolution, *GSA Today*, *8*, 1–7, 1998.

Condie, K. C., Episodic ages of greenstones: A key to mantle dynamics, *Geophys. Res. Lett.*, *22*, 2215–2218, 1995.

Condie, K. C., *Plate Tectonics and Crustal Evolution*, 282 pp., Butterworth-Heinemann, Woburn, Mass., 1997.

Condie, K. C., Episodic continental growth and supercontinents: A mantle avalanche connection, *Earth Planet. Sci. Lett.*, *163*, 97–108, 1998.

Condie, K. C., Episodic continental growth models: Afterthoughts and extensions, *Tectonophysics*, *322*, 153–162, 2000.

Cull, J. P., An appraisal of Australian heat-flow data, *BMR J. Aust. Geol. Geophys.*, *7*, 11–21, 1982.

Cull, J. P., and D. Conley, Geothermal gradients and heat flow in Australian sedimentary basins, *BMR J. Aust. Geol. Geophys.*, *8*, 329–337, 1983.

Cull, J. P., S. Y. O'Reilly, and W. L. Griffin, Xenolith geotherms and crustal models in eastern Australia, *Tectonophysics*, *192*, 359–366, 1991.

Davies, G. F., *Dynamic Earth, Plates, Plumes and Mantle Convection*, 458 pp., Cambridge Univ. Press, New York, 1999.

Davies, G. F., and J. W. Strebeck, Old continental geotherms: Constraints on heat production and thickness of continental plates, *Geophys. J. R. Astron. Soc.*, *69*, 623–634, 1982.

Decker, E. R., Thermal regimes of the Southern Rocky Mountains and Wyoming Basin in Colorado and Wyoming in the United States, *Tectonophysics*, *244*, 85–106, 1995.

De Smet, J., A. P. Van den Berg, and N. J. Vlaar, Early formation and long-term stability of continents resulting from decompression melting in a convecting mantle, *Tectonophysics*, *322*, 19–33, 2000.

Doin, M.-P., L. Fleitout, and U. Christensen, Mantle convection and stability of depleted and undepleted continental lithosphere, *J. Geophys. Res.*, *102*, 2771–2787, 1997.

Drury, M. J., Heat flow and heat generation in the Churchill Province of the Canadian Shield and their paleotectonic significance, *Tectonophysics*, *115*, 25–44, 1985.

Drury, M. J., and A. Taylor, Some new measurements of heat flow in the Superior Province of the Canadian Shield, *Can. J. Earth Sci.*, *24*, 1486–1489, 1987.

Drury, M. J., A. M. Jessop, and T. J. Lewis, The thermal nature of the Canadian Appalachian crust, *Tectonophysics*, *133*, 1–14, 1987.

Duchkov, A. D., and L. S. Sokolova, Thermal structure of Siberian lithosphere, in *Terrestrial Heat Flow and Geothermal Energy in Asia*,

edited by M. L. Gupta and M. Yamano, p. 281–298, Oxford and IBH, New Delhi, India, 1995.

Duchkov, A. D., S. V. Lysak, and V. T. Balobaev, *Thermal Field of Siberia Interiors* (in Russian), 196 pp., Nauka, Moscow, 1987.

Duchkov, A. D., V. T. Balobaev, and B. V. Volodko, Temperature, permafrost and radiogenic heat production in the Earth's crust of northern Asia (in Russian), *Proc. Inst. Geol. Geophys. Mineral.*, *821*, 144 pp., 1994.

Durrheim, R. J., and W. D. Mooney, Evolution of the Precambrian lithosphere: Seismological and geochemical constraints, *J. Geophys. Res.*, *99*, 15,359–15,374, 1994.

Eggler, D. H., On-craton and off-craton kimberlites and associated magmas: Relation to lithospheric thickness, *Geol. Soc. Am. Abstr. Programs*, *19*(7), 652, 1987.

Eggler, D. H., J. K. Meen, F. Welt, F. O. Dudas, K. P. Furlong, M. E. McCallum, and R. W. Carlson, Tectonomagmatism of the Wyoming Province, *Colo. Sch. Mines Q.*, *83*(2), 25–40, 1988.

Ekström, G., J. Tromp, and E. W. F. Larson, Measurements and global models of surface wave propagation, *J. Geophys. Res.*, *102*, 8137–8157, 1997.

England, P. C., E. R. Oxburgh, and S. W. Richardson, Heat refraction and heat production in and around granite plutons in north-east England, *Geophys. J. R. Astron. Soc.*, *62*, 439–455, 1980.

Ferguson, J., R. J. Arculus, and J. Joyce, Kimberlite and kimberlitic intrusives of southeastern Australia: A review, *BMR J. Austral. Geol. Geophys.*, *4*, 227–241, 1979.

Fountain, D. M., Is there a relationship between seismic velocity and heat production for crustal rocks?, *Earth Sci. Planet. Lett.*, *79*, 145–150, 1986.

Fountain, D. M., M. H. Salisbury, and K. P. Furlong, Heat production and thermal conductivity of rocks from the Pikwitonei-Sachigo continental cross-section, central Manitoba: Implications for the thermal structure of Archean crust, *Can. J. Earth Sci.*, *24*, 1583–1594, 1987.

Gao, S., T.-C. Luo, B.-R. Zhang, H.-F. Zhang, Y.-W. Han, Y.-K. Hu, and Z.-D. Zhao, Chemical composition of the continental crust as revealed by studies in east China, *Geochim. Cosmochim. Acta*, *62*, 1959–1975, 1998.

Goodwin, A. M., *Principles of Precambrian Geology*, 327 pp., Academic, San Diego, Calif., 1996.

Grand, S. P., Mantle shear structure beneath the Americas and surrounding oceans, *J. Geophys. Res.*, *99*, 11,591–11,621, 1994.

Griffin, W. L., F. L. Sutherland, and J. D. Hollis, Geothermal profile and crust-mantle transition beneath east-central Queensland: Volcanology, xenolith petrology and seismic data, *J. Volcanol. Geotherm. Res.*, *31*, 177–203, 1987.

Griffin, W. L., N. V. Sobolev, C. G. Ryan, N. P. Pokhilenko, T. T. Win, and E. S. Yefimova, Trace elements in garnets and chromites: Diamond formation in the Siberian lithosphere, *Lithos*, *29*, 235–256, 1993.

Griffin, W. L., F. V. Kaminsky, C. G. Ryan, S. Y. O. O'Reilly, T. T. Win, and I. P. Ilupin, Thermal state and composition of the lithospheric mantle beneath the Daldyn kimberlite field, Yakutia, *Tectonophysics*, *262*, 19–33, 1996.

Griffin, W. L., B. J. Foyle, C. G. Ryan, N. J. Pearson, S. Y. O'Reilly, R. Davies, K. Kivi, E. Van Achterbergh, and L. M. Natapov, Layered mantle lithosphere in the Lac de Gras Area, Slave Craton: Composition, structure and origin, *J. Petrol.*, *40*, 705–727, 1999.

Guillou, L., J.-C. Mareschal, C. Jaupart, C. Gariepy, G. Bienfait, and R. Lapointe, Heat flow, gravity and structure of the Abitibi belt, Superior Province, Canada: Implications for mantle heat flow, *Earth Planet. Sci. Lett.*, *122*, 103–123, 1994.

Guillou-Frottier, L., J.-C. Mareschal, C. Jaupart, C. Gariepy, R. Lapointe, and G. Bienfait, Heat flow variations in the Grenville Province, Canada, *Earth Planet. Sci. Lett.*, *136*, 447–460, 1995.

Guillou-Frottier, L., C. Jaupart, J.-C. Mareschal, C. Gariepy, G. Bienfait, L. Z. Cheng, and R. Lapointe, High heat flow in the Trans-Hudson Orogen, central Canadian Shield, *Geophys. Res. Lett.*, *23*, 3027–3030, 1996.

Gupta, M. L., Is the Indian Shield hotter than other Gondwana shields?, *Earth Planet. Sci. Lett.*, *115*, 275–285, 1993.

Gupta, M. L., and S. R. Sharma, Crustal thermal structure of Dharwar Craton, paper presented at 3rd Workshop on Status, Problems and Programmes in Indian Peninsular Shield, Inst. of Indian Peninsular Geol., Hyderabad, India, 1979.

Gupta, M. L., S. R. Sharma, A. Sundar, and S. B. Singh, Geothermal studies in the Hyderabad granitic region and the crustal thermal structure of the southern Indian Shield, *Tectonophysics*, *140*, 257–264, 1987.

Gupta, M. L., A. Sundar, and S. R. Sharma, Heat flow and heat generation in the Archean Dharwar cratons and implications for the southern Indian Shield geotherm and lithospheric thickness, *Tectonophysics*, *194*, 107–122, 1991.

Gupta, M. L., A. Sundar, S. R. Sharma, and S. B. Singh, Heat flow in the Bastar craton, central Inrian Shield: Implications for thermal characteristics of Proterozoic cratons, *Phys. Earth Planet. Inter.*, *78*, 23–31, 1993.

Hamza, V. M., Terrestrial heat flow in the alkaline intrusive complex of Pocos de Caldas, Brazil, *Tectonophysics*, *83*, 45–62, 1982a.

Hamza, V. M., Thermal structure of South American continental lithosphere during Archean and Proterozoic, *Rev. Brasil. Geocien.*, *12*, 149–159, 1982b.

Hart, R. J., L. O. Nicolaysen, and N. H. Gale, Radioelement concentrations in the deep profile through Precambrian basement of the Vredefort structure, *J. Geophys. Res.*, *86*, 10,639–10,652, 1981.

Hawkesworth, C. J., P. D. Kempton, N. W. Rogers, R. M. Ellam, and P. W. van Calsteren, Continental mantle lithosphere, and shallow level enrichment process in the Earth's mantle, *Earth Planet. Sci. Lett.*, *96*, 256–268, 1990.

Herzberg, C., Generation of plume magmas through time: An experimental perspective, *Chem. Geol.*, *126*, 1–16, 1995.

Hurter, S. J., and H. N. Pollack, Terrestrial heat flow in the Parana Basin, southern Brazil, *J. Geophys. Res.*, *101*, 8659–8671, 1996.

Jaeger, J. C., Heat flow and radioactivity in Australia, *Earth Planet. Sci. Lett.*, *8*, 285–292, 1970.

Jaupart, C., Horizontal heat transfer due to radioactivity contrasts: Causes and consequences of the linear heat flow relation, *Geophys. J. R. Astron. Soc.*, *75*, 411–435, 1983.

Jaupart, C., and J.-C. Mareschal, Thermal structure and thickness of continental roots, *Lithos*, *48*, 93–114, 1999.

Jaupart, C., J.-C. Mareschal, L. Guillou-Frottier, and A. Davaille, Heat flow and thickness of the lithosphere in the Canadian Shield, *J. Geophys. Res.*, *103*, 15,269–15,286, 1998.

Jessop, A. M., and T. J. Lewis, Heat flow and heat generation in the Superior Province of the Canadian Shield, *Tectonophysics*, *50*, 55–77, 1978.

Joeleht, A., and I. T. Kukkonen, Thermal properties of granulite facies rocks in the Precambrian basement of Finland and Estonia, *Tectonophysics*, *291*, 195–203, 1998.

Jones, M. Q. W., Heat flow and heat production in the Namaqua mobile belt, South Africa, *J. Geophys. Res.*, *92*, 6273–6289, 1987.

Jones, M. Q. W., Heat flow in the Witwatersrand Basin and environs and its significance for the South African Shield geotherm and lithosphere thickness, *J. Geophys. Res.*, *93*, 3243–3260, 1988.

Jones, M. Q. W., Heat flow anomaly in Lesotho: Implications for the southern boundary of the Kaapvaal Craton, *Geophys. Res. Lett.*, *19*, 2031–2034, 1992.

Jordan, T. H., Lateral heterogeneity and mantle dynamics, *Nature*, *257*, 745–750, 1975.

Jordan, T. H., Mineralogies, densities and seismic velocities of garnet lherzolites and their geophysical implications, in *The Mantle Sample: Inclusions in Kimberlite and Other Volcanics*, edited by F. R. Boyd and H. O. A. Meyer, pp. 1–14, AGU, Washington, D. C., 1979.

Jordan, T. H., Structure and formation of the continental tectosphere, *J. Petrol.*, *29*, 11–37, 1988.

Judge, A., Terrestrial heat flow in the Grenville Province of the Canadian Shield, *Eos Trans. AGU*, *59*(12), 1028, 1978.

Kennedy, C. S., and G. C. Kennedy, The equilibrium boundary between graphite and diamond, *J. Geophys. Res.*, *81*, 2467–2470, 1976.

Kern, H., and S. Siegesmund, A test of the relationship between seismic velocity and heat production for crustal rocks, *Earth Sci. Planet. Lett.*, *92*, 89–94, 1989.

Ketcham, R. A., Distribution of heat-producing elements in the upper and middle crust of southern and west central Arizona: Evidence from the core complexes, *J. Geophys. Res.*, *101*, 13,611–13,632, 1996.

Kopylova, M. G., J. K. Russell, and H. Cookenboo, Petrology of peridotite and pyroxenite xenoliths from the Jericho kimberlite: implications for the thermal state of the mantle beneath the Slave Craton, northern Canada, *J. Petrol.*, *40*, 79–104, 1999.

Kjarsgaard, B. A., and T. D. Peterson, Kimberlite-derived ultramafic xenoliths from the diamonds stability field: A new Cretaceous geo-

therm for Somerset Island, Northwest Territories, in *Current Research*, *Part B*. *Pap. Geol. Surv. Can*., *92-1B*, 1–6, 1992.

Kremenetsky, A. A., S. Y. Milanovsky, and L. N. Ovchinnikov, A heat generation model for continental crust based on deep drilling in the Baltic Shield, *Tectonophysics*, *159*, 231–246, 1989.

Kukkonen, I. T., Terrestrial heat flow and radiogenic heat production in Finland, the central Baltic Shield, *Tectonophysics*, *164*, 219–230, 1989.

Kukkonen, I. T., and P. Peltonen, Xenolith-controlled geotherm for the central Fennoscandian Shield: implications for lithosphere-asthenosphere relations, *Tectonophysics*, *304*, 301–315, 1999.

Kutas, R. I., V. A. Tsviaschenko, and I. N. Korchagin, *Modelling Thermal Field of the Continental Lithosphere* (in Russian), 191 pp., Naukova Dumka, Kiev, Russia, 1989.

Lachenbruch, A. H., Crustal temperature and heat production: Implications of the linear heat flow relation, *J. Geophys. Res*., *75*, 3291–3300, 1970.

Lachenbruch, A. H., and P. Morgan, Continental extension, magmatism and elevation; formal relations and rules of thumb, *Tectonophysics*, *174*, 39–62, 1990.

Lachenbruch, A. H., and J. H. Sass, Heat flow in the United States and the thermal regime of the crust, in *The Earth's Crust: Its Nature and Physical Properties*, *Geophys. Monogr. Ser*., vol. 20, edited by J. G. Heacock, pp. 626–675, AGU, Washington, D. C., 1977.

Le Pichon, X., P. Henry, and B. Goffe, Uplift of Tibet: From eclogites to granulites—Implications for the Andean Plateau and the Variscan belt, *Tectonophysics*, *273*, 57–76, 1997.

Lithgow-Bertelloni, C., and P. G. Silver, Dynamic topography, plate driving forces and the African superswell, *Nature*, *395*, 269–272, 1998.

Ludden, J. N. (Ed.), The Abitibi-Grenville Lithoprobe transect seismic reflection results, part 1, The western Grenville Province and Pontiac subprovince, *Can. J. Earth Sci*., *32*, 97–272, 1995.

Mackenzie, J. M., and D. Canil, Thermal state of the lower crust and upper mantle of the Archean Slave Province, NWT, Canada: A xenolith study, paper presented at MIT-Harvard Workshop on Continental Roots, Harvard Univ., Cambridge, Mass., Oct. 1997.

Malmquist, D., S. A. Larson, O. Landstrom, and G. Lind, Heat flow and heat production from the Malinsbo granite, central Sweden, *Bull. Geol. Inst. Univ. Uppsala*, *9*, 137–152, 1983.

Mareschal, J.-C., Downward continuation of heat flow density data and thermal regime in eastern Canada, *Tectonophysics*, *194*, 349–356, 1991.

Mareschal, J.-C., C. Pinet, C. Gariepy, C. Jaupart, G. Bienfait, G. Dalla Coletta, J. Jolivet, and R. Lapointe, New heat flow density and radiogenic heat production data in the Canadian Shield and the Quebec Appalachians, *Can. J. Earth Sci*., *26*, 845–852, 1989.

Mareschal, J.-C., C. Jaupart, L. Z. Cheng, F. Rolandone, C. Gariepy, G. Bienfait, L. Guillou-Frottier, and R. Lapointe, Heat flow in the Trans-Hudson Orogen of the Canadian Shield: Implications for Proterozoic continental growth, *J. Geophys. Res*., *104*, 29,007–29,024, 1999.

Mareschal, J.-C., C. Jaupart, C. Gariepy, L. Z. Cheng, L. Guillou-Frottier, G. Bienfait, and R. Lapointe, Heat flow and deep thermal structure near the edge of the Canadian Shield, *Can. J. Earth Sci*., *37*, 399–414, 2000a.

Mareschal, J.-C., A. Porier, F. Rolandone, G. Bienfait, C. Gariépy, R. Lapointe, and C. Jaupart, Low mantle heat flow at the edge of the North American continent, Voisey Bay, Laborador, *Geophys. Res. Lett*., *27*, 823–826, 2000b.

Martin, H., The mechanisms of petrogenesis of the Archean continental crust—Comparison with modern processes, *Lithos*, *30*, 373–388, 1993.

Martin, H., Archean gray gneisses and the genesis of continental crust, in *Archean Crustal Evolution*, edited by K. C. Condie, pp. 205–260, Elsevier Sci., New York, 1994.

McLennan, S. M., and S. R. Taylor, Heat flow and the chemical composition of continental crust, *J. Geol*., *104*, 377–396, 1996.

McNutt, M., Flexure reveals great depth, *Nature*, *343*, 205–260, 1990.

Mechie, J., K. Fuchs, and R. Altherr, The relationship between seismic velocity, mineral composition and temperature and pressure in the upper mantle—With an application to the Kenya Rift and its eastern flank, *Tectonophysics*, *236*, 453–464, 1994.

Menzies, M. A., F. Weiming, and M. Zhang, Paleozoic and Cenozoic lithoprobes and the loss of >120 km of Archean lithosphere, Sino-Korean craton, China, in *Magmatic Processes and Plate Tectonics*, edited by H. M. Prichard et al., *Geol. Soc. Spec. Publ*., *76*, 71–81, 1993.

Mooney, W. D., G. Laske, and T. G. Masters, CRUST 5.1: A global crustal model at 5° × 5°, *J. Geophys. Res*., *103*, 727–747, 1998.

Morgan, P., Crustal radiogenic heat production and the selective survival of ancient continental crust, *Proc. Lunar Planet. Sci. Conf. 15th*, Part 2, *J. Geophys. Res*., suppl., *90*, C561–C570, 1985.

Nataf, H.-C., and Y. Ricard, 3SMAC: An a priori tomographic model of the upper mantle based on geophysical modeling, *Phys. Earth Planet. Inter*., *95*, 101–122, 1996.

Negi, J. G., O. P. Pandey, and P. K. Agrawal, Super-mobility of hot Indian lithosphere, *Tectonophysics*, *131*, 147–156, 1986.

Negi, J. G., P. K. Agrawal, and O. P. Pandey, Large variation of Curie depth and lithosphere thickness beneath the Indian subcontinent and a case for magnetothermometry, *Geophys. J. R. Astron. Soc*., *88*, 763–775, 1987.

Nelson, D., Granite-greenstone crust formation on the Archean Earth: A consequence of two superimposed processes, *Earth Planet. Sci. Lett*., *158*, 109–119, 1998.

Nicolaysen, L. O., R. J. Hart, and N. H. Gale, The Vredefort radioelement profile extended to supracrustal strata at Carletonville, with implications for continental heat flow, *J. Geophys. Res*., *86*, 10,653–10,661, 1981.

Nyblade, A. A., Heat flow across the East African Plateau, *Geophys. Res. Lett*., *24*, 2083–2086, 1997.

Nyblade, A. A., Heat flow and the structure of Precambrian lithosphere, *Lithos*, *48*, 81–91, 1999.

Nyblade, A. A., and H. N. Pollack, A global analysis of heat flow from Precambrian terrains: Implications for the thermal structure of Archean and Proterozoic lithosphere, *J. Geophys. Res*., *98*, 12,207–12,218, 1993.

Nyblade, A. A., H. N. Pollack, D. L. Jones, F. Podmore, and M. Mushayandebvu, Terrestrial heat flow in east and southern Africa, *J. Geophys. Res*., *95*, 17,371–17,384, 1990.

O'Hara, M. J., Is there an Icelandic mantle plume?, *Nature*, *253*, 708–710, 1975.

O'Reilly, S. Y., and W. L. Griffin, A xenolith-derived geotherm for southeastern Australia and its geophysical implications, *Tectonophysics*, *111*, 41–63, 1985.

Pasquale, V., C. Cabella, and M. Verdoya, Deep temperatures and lithospheric thickness along the European Geotraverse, *Tectonophysics*, *176*, 1–11, 1990.

Pasquale, V., M. Verdoya, and P. Chiozzi, Lithospheric thermal structure in the Baltic Shield, *Geophys. J. Int*., *106*, 611–620, 1991.

Pearson, D. G., The age of continental roots, *Lithos*, *48*, 171–194, 1999.

Pearson, D. G., R. W. Carlson, S. B. Shirey, F. R. Boyd, and P. H. Nixon, Stabilisation of Archaean lithospheric mantle: A Re-Os isotope study of peridotite xenoliths from the Kaapvaal Craton, *Earth Planet. Sci. Lett*., *134*, 341–357, 1995.

Pinet, C., and C. Jaupart, The vertical distribution of radiogenic heat production in the Precambrian crust of Norway and Sweden: Geothermal implications, *Geophys. Res. Lett*., *14*, 260–263, 1987.

Pinet, C., C. Jaupart, J.-C. Mareschal, C. Gariépy, G. Bienfait, and R. Lapointe, Heat flow and structure of the lithosphere in the eastern Canadian Shield, *J. Geophys. Res*., *96*, 19,941–19,963, 1991.

Pokhilenko, N. P., N. V. Sobolev, F. R. Boyd, D. G. Pearson, and N. Shimizu, Megacrystalline pyrope peridotites in the lithosphere of the Siberian Platform: Mineralogy, geochemical peculiarities and the problem of their origin, *Russ. Geol. Geophys*., *34*(1), 56–67, 1993.

Polet, J., and D. L. Anderson, Depth extent of cratons as inferred from tomographic studies, *Geology*, *23*, 205–208, 1995.

Pollack, H. N., Cratonization and thermal evolution of the mantle, *Earth Planet. Sci. Lett*., *80*, 175–182, 1986.

Pollack, H. N., and D. S. Chapman, On the regional variation of heat flow, geotherms and lithospheric thickness, *Tectonophysics*, *38*, 279–296, 1977.

Pollack, H. N., S. Hurter, and J. R. Johnson, The new global heat flow data compilation, *Eos Trans. AGU*, *71*, 1604, 1990.

Pollack, H. N., S. J. Hurter, and J. R. Johnson, Heat flow from the Earth's interior: Analysis of the global data set, *Rev. Geophys*., *31*, 267–280, 1993.

Polyakov, A. I., N. S. Muravieva, and V. G. Senin, Partial melting of the upper mantle in the Baikal rift (from studies of glasses in lherzolite nodules and megachrysts) (in Russian), *Dokl. Akad. Nauk SSSR*, *300*(1), 208–213, 1988.

Powell, W. G., D. S. Chapman, N. Balling, and A. E. Beck, Continental

heat-flow density, in *Handbook of Terrestrial Heat-Flow Density Determination*, edited by R. Haenel, L. Rybach, and L. Stegena, pp. 167–222, Kluwer Acad., Norwell, Mass., 1988.

Rao, R. U. M., and A. M. Jessop, A comparison of the thermal character of shields, *Can. J. Earth Sci*., *12*, 347–360, 1975.

Rao, R. U. M., G. V. Rao, and H. Narain, Radioactive heat generation and heat flow in the Indian Shield, *Earth Planet. Sci. Lett*., *30*, 57–64, 1976.

Richardson, S. H., J. W. Harris, and J. J. Gurney, Three generations of diamonds from old continental mantle, *Nature*, *366*, 256–258, 1993.

Ritsema, J., and H. van Heijst, New seismic model of the upper mantle beneath Africa, *Geology*, *28*, 63–66, 2000.

Ritzwoller, M. H., and A. L. Levshin, Eurasian surface wave tomography: Group velocities, *J. Geophys. Res*., *103*, 4839–4878, 1998.

Rogers, J. J. W., and E. J. Callahan, Radioactivity, heat flow, and rifting of the Indian continental crust, *J. Geol*., *95*, 829–836, 1987.

Roy, R. F., D. D. Blackwell, and F. Birch, Heat generation of plutonic rocks and continental heat flow provinces, *Earth Planet. Sci. Lett*., *5*, 1–12, 1968.

Rozen, O. M., Heat generation of the crust of the Anabar shield and the problems of formation of the lower crust of the continents (in Russian), *Geol. Geofiz*., no. 12, 22–29, 1992.

Rudnick, L. R., and D. M. Fountain, Nature and composition of the continental crust: a lower crustal perspective, *Rev. Geophys*., *33*, 267–309, 1995.

Rudnick, L. R., and A. A. Nyblade, The thickness and heat production of Archean lithosphere: Constraints from xenolith thermobarometry and surface heat flow, in *Mantle Petrology: Field Observations and High Pressure Experimentation: A Tribute to Francis R. (Joe) Boyd*, edited by Y. Fei, C. M. Bertka, and B. O. Mysen, *Chem. Soc. Spec. Publ*., *6*, 3–12, 1999.

Rudnick, L. R., and T. Presper, Geochemistry of intermediate to high-pressure granulites, in *Granulites and Crustal Evolution*, edited by D. Vielzeuf and P. Vidal, pp. 523–550, Kluwer Acad., Norwell, Mass., 1990.

Rudnick, L. R., W. F. McDonough, and R. J. O'Connel, Thermal structure, thickness and composition of continental lithosphere, *Chem. Geol*., *145*, 395–411, 1998.

Russell, J. K., and M. G. Kopylova, A steady-state conductive geotherm for the north central Slave, Canada: Inversion of petrological data from the Jericho kimberlite pipe, *J. Geophys. Res*., *104*, 7089–7102, 1999.

Ryan, C. G., W. L. Griffin, and N. J. Pearson, Garnet geotherms: Pressure-temperature data from Cr-pyrope garnet xenocrysts in volcanic rocks, *J. Geophys. Res*., *101*, 5611–5625, 1996.

Rybach, L., and G. Buntebarth, The variation of heat generation, density and seismic velocity with rock type in the continental lithosphere, *Tectonophysics*, *103*, 335–344, 1984.

Sass, J. H., and J. C. Behrendt, Heat flow from the Liberian Precambrian Shield, *J. Geophys. Res*., *85*, 3159–3162, 1980.

Sass, J. H., and A. H. Lachenbruch, The thermal regime of the Australian continental crust, in *The Earth—Its Origin, Structure and Evolution*, edited by M. W. McElhinny, pp. 301–352, Academic, San Diego, Calif., 1979.

Sass, J. H., J. C. Jaeger, and R. J. Munroe, Heat flow and near-surface radioactivity in the Australian continental crust, *U.S. Geol. Surv. Open File Rep*., *76-250*, 1976.

Sato, H., I. S. Sacks, and T. Murase, The use of laboratory velocity data for estimating temperature and partial melt fraction in the low-velocity zone: Comparison with heat flow and electrical studies, *J. Geophys. Res*., *94*, 5689–5704, 1989.

Scharmeli, G., Identification of radioactive thermal conductivity in olivine up to 25 kbar and 1500 K, in *Proceedings of the 6th Airapt Conference*, edited by K. D. Timmerhauf and M. S. Barber, pp. 60–74, Plenum, New York, 1979.

Schatz, J. F., and G. Simmons, Thermal conductivity of Earth minerals at high temperatures, *J. Geophys. Res*., *77*, 6966–6983, 1972.

Schmidberger, S. S., and D. Francis, Nature of the mantle roots beneath the North American Craton: Mantle xenolith evidence from Somerset Island kimberlites, *Lithos*, *48*, 195–216, 1999.

Sclater, J. G., C. Jaupart, and D. Galson, The heat flow through oceanic and continental crust and the heat loss of the Earth, *Rev. Geophys*., *18*, 269–311, 1980.

Seipold, U., Depth dependence of thermal transport properties for typical crustal rocks, *Phys. Earth Planet. Inter*., *69*, 299–303, 1992.

Shaw, D. M., J. J. Cramer, M. D. Higgins, and M. G. Truscott, Composition of the Canadian Precambrian shield and the continental crust of the Earth, in *Nature of the Lower Continental Crust*, edited by J. B. Dawson et al., *Geol. Soc. Spec. Publ*., *24*, 275–282, 1986.

Simons, F. J., A. Zielhuis, and R. D. van der Hilst, The deep structure of the Australian continent from surface wave tomography, *Lithos*, *48*, 17–43, 1999.

Singh, R. N., and J. G. Negi, High Moho temperature in the Indian Shield, *Tectonophysics*, *82*, 299–306, 1982.

Swanberg, C. A., M. D. Chessman, and G. Simmons, Heat flow-heat generation studies in Norway, *Tectonophysics*, *23*, 31–48, 1974.

Taylor, S. R., and S. M. McLennan, *The Continental Crust: Its Composition and Evolution*, 312 pp., Blackwell, Malden, Mass., 1985.

Turcotte, D. L., and G. Schubert, *Geodynamics*, 347 pp., John Wiley, New York, 1982.

Van der Hilst, R., B. L. N. Kennett, and T. Shibutani, Upper mantle structure beneath Australia from portable array deployments, in *Structure and Evolution of the Australian Continent*, *Geodyn. Ser*., vol. 26, edited by J. Braun et al., pp. 39–57, AGU, Washington, D. C., 1998.

van der Lee, S., and G. Nolet, Upper mantle *S* velocity structure of North America, *J. Geophys. Res*., *102*, 22,815–22,838, 1997.

Van Heijst, H. J., and J. Woodhouse, Measuring surface wave overtone phase velocities using a mode-branch stripping, *Geophys. J. Int*., *145*, 209–230, 1997.

Vernik, L. I., N. E. Galdin, and L. I. Kagalova, A construction of deep petrophysical models of ancient shields (an example of the eastern part of the Baltic Shield) (in Russian), in *Petrophysical Studies in Shields and Platforms*, edited by N. B. Dortman, pp. 17–23, Geol. Inst., Kola Branch, USSR Acad. of Sci., Apatity, Russia, 1985.

Vitorello, I., V. M. Hamza, and H. N. Pollack, Terrestrial heat flow in the Brazilian highlands, *J. Geophys. Res*., *85*, 3778–3788, 1980.

Vlaar, N. J., P. E. Keken, and A. P. Van den Berg, Cooling of the Earth in the Archean: Consequences of pressure-release melting in a hotter mantle, *Earth Planet. Sci. Lett*., *121*, 1–18, 1994.

Wang, C. J. (Ed.), *Geothermics in China*, 300 pp., Seismol. Press, Beijing, 1996.

Weaver, B. L., and J. Tarney, Empirical approach to estimating the composition of the continental crust, *Nature*, *310*, 575–577, 1984.

Yale, L. B., and S. J. Carpenter, Large igneous provinces and giant dyke swarms: Proxies for supercontinent cyclicity and mantle convection, *Earth Planet. Sci. Lett*., *163*, 109–122, 1998.

Zhang, Y.-S., and T. Tanimoto, High-resolution global upper mantle structure and plate tectonics, *J. Geophys. Res*., *98*, 9793–9823, 1993.

I. M. Artemieva, Department of Earth Sciences, Uppsala University, Villavagen 16, S-75236 Uppsala, Sweden. (iartem@geofys.uu.se)

W. D. Mooney, U.S. Geological Survey, 345 Middlefield Road, MS 977, Menlo Park, CA 94025. (mooney@usgs.gov)

(Received January 7, 2000; revised August 28, 2000;
accepted November 29, 2000.)